Petri Forsström

PSK-31 Receiver

Design, Analysis and Assembly

Helsinki Metropolia University of Applied Sciences

Bachelor Degree

Electronics

Thesis

April 2014

Helsinki Metropolia University of Applied Sciences

Acknowledgements

I would like to acknowledge the guidance and support of my instructor, Senior Lecturer Thierry Baills, in this project and throughout my studies in Metropolia UAS. His optimism, expertise and inspiring teaching style are rarely met and continue to benefit the students of electronics.

I would like to express my special thanks to Principal Lecturer Kari Salmi for his helpful guidance in PCB design for this project and for taking an interest in my studies during the degree program. Similarly, I thank Lecturer Petri Valve for his guidance in the English studies and for reviewing this thesis. I would also like to extend my gratitude for Laboratory Engineer Teemu Mahrberg whose helpfulness has benefited me greatly in several occasions.

I take this opportunity to thank also my classmate and friend, Mr. Peter Kijanga for his empowering, positive attitude that inspired me during the long writing process.

Finally, my wife Hanna whose support and understanding I value the most. Thank you.

In Helsinki on 25 April 2014

Author Title Number of Pages Date	Petri Forsström PSK-31 Receiver's Design, Analysis and Assembly 43 pages + 4 appendices 25 Apr 2014
Degree	Bachelor of Engineering
Degree Programme	Electronics
Instructor	Thierry Baills, Senior Lecturer

This thesis introduces an electronic design for a PSK-31 radio receiver. The goal of the study was to construct a PSK-31 receiver for down-converting a high frequency carrier spectrum to an audible centre frequency and to feed the down-converted signal into a computer soundcard for digital signal processing.

In this report, the PSK-31 radio receiver design is explained through methods of analysis and synthesis. In the analysis, the circuit is divided into individual, functional blocks, where relevant theory is introduced to explain the effects of the circuit on the input signal. As the several blocks are introduced one by one, the reader gains a complete view on how the receiver is constructed and what the main factors are to be considered. In the synthesis, the circuit is studied as a complete design. The redrawn circuit diagram and the printed circuit board layout are represented in the report.

The goal of the project was achieved in laboratory testing, using an external signal generator as a signal source. The down-converted signal was observed in the digital signal processing interface. Acquiring a reception of an actual PSK-31 signal would have required more freedom in picking precise value filter components. The design itself was considered successful and provides a good basis for further development.

Keywords	PSK-31, PSK31, BPSK, Receiver

Tekijä Otsikko Sivumäärä Aika	Petri Forsström PSK-31 vastaanottimen suunnittelu, analyysi ja kokoaminen 43 sivua + 4 liitettä 25.4.2014
Tutkinto	Insinööri (AMK)
Koulutusohjelma	Elektroniikka
Ohjaaja	lehtori Thierry Baills

Tämän insinöörityön päämääränä oli tutkia PSK-31 radiovastaanottimen teoriaa ja rakentaa vastaanottimen prototyyppi. Tarkoituksena oli alassekoittaa korkeataajuuksinen kantoaalto korvinkuultavalle taajuudelle. Alassekoitettu signaali tuli syöttää tietokoneen äänikortille digitaalista signaalin käsittelyä ja kartoitusta varten.

Tämä insinöörityö käsitteli PSK-31 radiovastaanottimen elektroniikkasuunnittelun analyysin ja synteesin sekä vastaanottimen piirilevysuunnittelun piirikaaviosta prototyyppiin. Analyysissä vastaanotinpiiri jaettiin osakokonaisuuksiin, joiden roolit signaalin muokkauksessa selvitettiin teoreettisin menetelmin. Synteesissä vastaanotinpiirin toimintaa tarkasteltiin kokonaisuutena ja tutkittiin piirin aiheuttamaa sisääntulosignaalin muutosta ulostulosignaalin mittauksien avulla.

Projektin päämäärät saavutettiin laboratoriokokeissa käyttämällä signaalin lähteenä ulkoista signaaligeneraattoria. Alassekoitettu signaali todettiin tietokoneohjelman avulla. Todellisen PSK-31 signaalin vastaanottamiseksi piirisuunnittelussa olisi ollut tarpeen mahdollisuus valita vapaammin suodattimissa käytettyjen komponenttien arvot. Vastaanottimen prototyypin suunnittelutyö katsottiin onnistuneeksi ja mahdollistavan PSK-31 vastaanottimen jatkokehittelyn.

Avainsanat	PSK-31, PSK31, BPSK, Vastaanotin

Contents

Abbreviations

PSK	Phase-Shift Keying (modulation method)
PCB	Printed circuit board
RTTY	Radioteletype (mode of communication)
DSP	Digital signal processing
BPSK	Binary Phase-Shift Keying (modulation scheme)
$psk(t)$	PSK modulated signal
$s(t)$	Signal
QPSK	Quadrature Phase-Shift Keying (modulation scheme)
G5RV	A dipole antenna
UHF	Ultra High Frequency
RF	Radio Frequency
HF	High Frequency
λ/2	Half wave dipole (antenna type)
SO239	SO239 type connector
x_c	Carrier signal
$A(t)$	Instantaneous amplitude
ω_c	Carrier signal frequency
ϕ(t)	Instantaneous phase deviation
$m(t)$	Message signal
x_{LO}	Local oscillator signal
x_{IF}	Intermediate signal
$x_s(t)$	Processed signal
ω_0	Original frequency
ω_{IF}	Intermediate frequency
ω_{img}	Image frequency
IF	Intermediate Frequency (mixer output)
SMA	SubMiniature version A (connector)
LNA	Low Noise Amplifier
IC	Integrated Circuit

1 Introduction

This thesis aims to explain the phenomena affecting efficient and reliable information transfer via wireless medium by introducing an analysis of a PSK-31 receiver circuit. The ultimate goal of the project was to produce a functioning PSK-31 receiver for Metropolia UAS's teaching purposes.

The PSK-31 receiver design, covered in this thesis is based on a design introduced in the Nutz&Volts magazine [1]. The original article covers the circuit design in a very general way and enables the reader to construct the circuit without the need for deeper understanding of the receiver's internal functions. This study aims to explain the PSK-31 receiver circuit from a design point-of-view and provides explanations for the key elements in the receiver.

The study includes a theoretical step-by-step analysis of the circuit, from the input to the output. The analysis is introduced by utilizing methods of circuit analysis and references to several calculations, simulations and graphs to support the component selections and the circuit board design. The calculated results are used to compare the theory to the practical measurements. The explanatory manner in which the report is written gives the reader the possibility to repeat the project.

Schematic, printed circuit board (PCB) layout and the bill of materials of the project are found in appendices A, B and C. Appendix D provides additional information concerning the skywave propagation of electromagnetic waves and an explanation of how a transmitter with a low power output can be utilized to reach transmissions over intercontinental distances.

2 Theory and Operation

2.1 Description and Origins

PSK-31 is a communication method, developed by the English radio amateur operator Peter Martinez (call sign G3PLX) in the late 90's. The basic idea was to develop a new mode between the high-end data-transfer techniques and the traditional radioteletype (RTTY) mode of the 1960's. The problem, when utilizing the modern modes to live communications is their dependence on heavy error-correction systems that causes delays in both ends of the radio link. The high data rates of the modern systems are extravagant for keyboard typed information exchange between human interpreters, where the possible errors in the data can be interpreted from the context of the subject. The properties that do matter in radio amateurs communication include the fluency of the real-time communication with minimal delays and the possibility to listen to multiple channels freely without the need for a data link. PSK-31 is closer to traditional RTTY modes that the modern modes and therefore PSK-31 can be considered an updated version of RTTY rather than a simplified version of the modern modes. [2]

PSK-31 uses so called Varicode as the digital modulator to include the message information as phase variations of the high frequency carrier signal. Varicode is very similar to Morse code but is optimized to suit the modern digital signal processing systems (DSP), rather than the human interpretative Morse code. Where Morse code uses distinctive amount of bits for the two possible code-elements (namely dash, 3-bit and dot, 1-bit), Varicode is unconfined by any distinctive amount of bits per a code-element. This enables more efficient modulation of the carrier wave and a need for a narrower bandwidth, which is one of the key advantages of PSK-31 compared to other conventional modes. As with Morse code, the code-length of each symbol is optimized, so that the most common letters, appearing in a typical written text, contains less bits that the more uncommon letters. The optimization of the code-lengths and the typical typing speed on a keyboard sums up to a bit-rate of about 32 bit per second. This indicates a typing speed of 50 words per minute. In Varicode, the average code-length per symbol is 6.5 bits. This includes the gap between the characters which is indicated by transmitting two consecutive zeroes after the actual symbol. When the transmitter is in idle mode, a continuous set of zeroes is transmitted. The zeroes are used, addition to the gaps, to synchronize the transmitter and the receiver so that the receiver "knows" to expect a code string. This is done by having the 0 state of Varicode as a reversal

phase of 180 degree and 1 state as the natural phase of the carrier signal. The comparison of Morse code and Varicode is shown in figure 1 with the word "ten" formulated with both methods. [2]

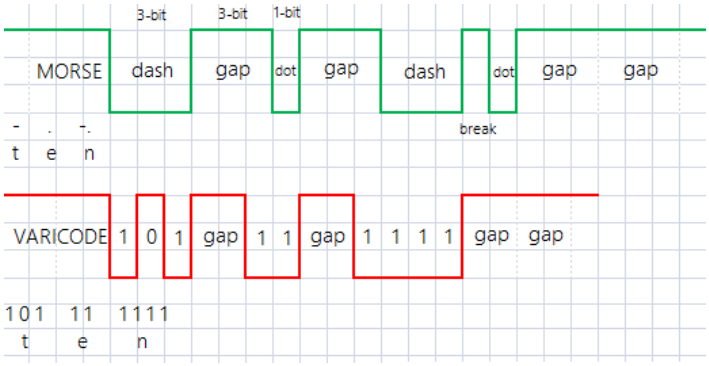

figure 1, Morse Code versus Varicode

The self-synchronization can be achieved by utilizing the knowledge of the modulation scheme. As for a modulation scheme, PSK-31 uses a binary phase-shift keying (BPSK) which means that the phase-shift of the carrier is modified with two states (1 and 0) that shift the phase of the carrier between 0 degrees and 180 degrees. Addition to the phase modulation, BPSK has an amplitude modulation component which can be used to synchronize the receiver to the transmitter. The operation of the synchronization is based on the idea that the receiver compares the already received bit to the incoming bit and in case of consecutive zeroes; it means that either there is a gap between the characters or the transmitter is in idle mode. In either case, the receiver can expect a code-element to appear and synchronize itself with the incoming data. An example of an amplitude modulation component and the phase shift is shown in figure 2, where the consecutive zeros, injecting the phase shifts of 180 degrees, can be seen on the left. As the first bit with state 1 is noted, no phase shift occurs which is also the case in the following bit. After the two 1's a zero bit is introduced and again the carrier changes it phase. The phase shift is illustrated in the close-up picture of figure 2. [2]

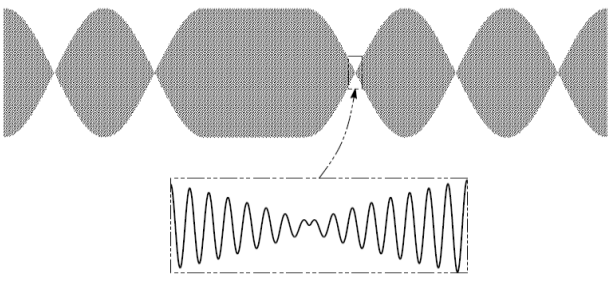

figure 2, BPSK modulation, Synchronization

Because of its simplicity, the method was widely accepted by radio amateurs around the world soon after its "official" introduction in 1999. Utilizing the soundcard technology of a normal desktop computer or a laptop makes the system affordable and easy to access. Intercontinental communication distances of thousands of kilometers can be achieved between the transmitter and the receiver. The good signal propagation is due to the phenomena where the carrier wave's energy reacts with particles in the ionosphere, causing reflections and refractions which again transfer the signal towards the surface of the earth. [3] See appendix D for more information on signal propagation.

In telecommunication, PSK refers to a modulation method called phase-shift keying. Modulation means altering the properties of one signal with another to gain advantages in propagation, processing, to enable encryption of vulnerable data and to have robust error resistance and low power consumption. In phase-shift keying a high frequency signal, of sinusoidal form, is modulated with the wanted message signal. A new signal called a carrier signal is produced which possess the frequency of the original high frequency signal and carries the message information within its phase variations.

The number 31 in PSK-31 refers to baud rate (symbols per second). This means a possibility to transmit 31 phase variations per seconds, which again means the amount of states (0 or 1) that can be injected into the carrier wave. This becomes the frequency envelope when presented in frequency domain and gives the bandwidth of approximately 31Hz. This correlates to the typing speed of 50 words per minute on a standard keyboard. [3]

2.2 Modulation Schemes

In PSK, the modulation is done by altering the phase of the carrier signal. PSK modulated signals can have two phase variations or more, depending on the application and the environment acting as the information transfer medium. figure 3 illustrate the most simple form of PSK where the high frequency carrier wave $psk(t)$ has been modulated with the digital signal $s(t)$. The carrier wave performs a 180 degree phase shift every time the digital signal changes its state.

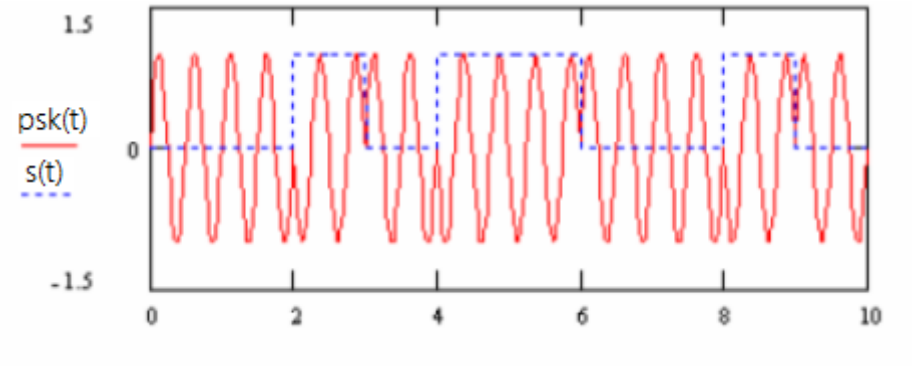

figure 3, Binary Phase-Shift Keying

The two most common PSK schemes are called a BPSK (Binary phase-shift keying), with two phase variations and QPSK (Quadrature phase-shift keying), with four phase variations. The BPSK modulation example shown in figure 3 operates according to equation 1 shown below and indicates a phase shift of 180 degrees at the moment of state change.

$$psk(t) = \begin{cases} \sin(2\pi ft) & for\ bit\ 0 \\ \sin(2\pi ft + \pi) & for\ bit\ 1 \end{cases} \quad (1)$$

Implementations of the different schemes have different advantages. The most obvious difference between the schemes is the number of phase variations. Systems requiring high speed transmissions favor QPSK scheme but require the error correction equipment, whereas applications such as PSK-31, designed for amateur use, utilizes the BPSK which has lower data rate but better error rejection properties. The difference in data rates comes from the fact that with QPSK the message signal can be used to modulate the carrier wave with higher efficiency than with BPSK. This is because of the four possible phase variations compared to the two phase variations of the BPSK. This means that with QPSK more data can be included into a smaller space in time. The downside of a higher data rate is its vulnerability to errors as the signal propagates through the air medium. The propagation path is not ideal but injects a certain amount of errors into the signal. As the four phases are closer to each other than in the BPSK scheme, the possibility of errors in the reception end is higher.

The two different schemes can be expressed with so called constellation diagrams. Constellation diagrams for BPSK and QPSK are shown in figure 4.

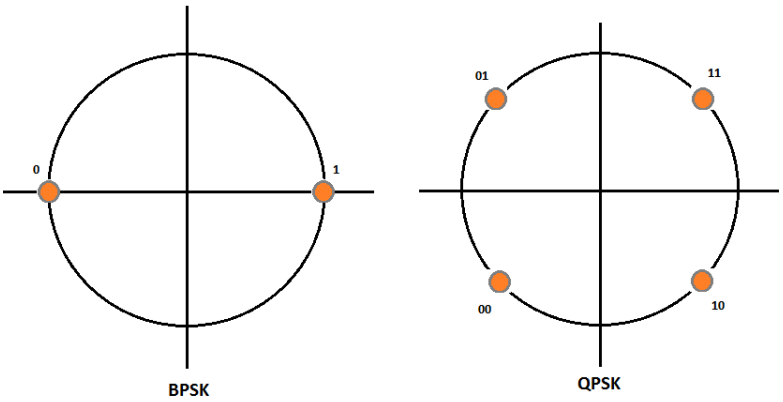

figure 4, Constellation diagrams of BPSK and QPSK

In BPSK scheme, the phase difference of states is 180 degrees (π in radians), meaning that the modulation induces always either a 0 degree or a 180 degree phase shift to appear in the carrier wave when the state of the message signal changes. Because only two possible phase shifts exist, the logical states can be only 0 or 1, resulting high error resistance but relatively low data rate. In the case of QPSK, there are four possible phase variations having 90 degree ($^{\pi}/_{2}$ radians) difference that start from 45 degrees ($^{\pi}/_{4}$) onwards, resulting four possible logical states, 00, 01, 10, 11. This means higher data rate. Having the states closer to each other phase wise, rises the chance of erroneous data read because the receiver is more likely to map a wrong symbol if the phase variation is not located at the exact point but between two points in the constellation diagram. Increase in the amount of states leads to the need for more sophisticated error correction equipment, which again means higher expenses.

PSK-31 is designed for radio amateur use only and thus, a BPSK scheme is the logical choice for the system. The benefits of operating with relatively simple, affordable equipment and having high error resistance originated from the scheme itself are properties that make PSK-31 so popular.

In a standard PSK-31 system, the modulation and the demodulation are performed by the computer's digital signal processing circuitry. In demodulation, the computer software maps the phase variations to binary code digits which again are mapped to represent symbols that make up the message in the user interface.

2.3 PSK-31 System Overview

A communication system requires always a transmitter and a receiver. In case the information is sent as electromagnetic waves via wireless medium, the distance between the two participants is usually large and good antennas are needed at both ends. The transmitter and the receiver units are placed between the user interfaces and the antennas, to provide the required electronics to convert the signal into a form that can efficiently propagate through the medium between the two participants. The basic set-up of PSK-31 system is illustrated in figure 5.

figure 5, Wireless transmitter-receiver system

The operation of the system can be illustrated with a block diagram where the functions of each block are placed in the correct position, relative to the data flow and conversions. A general block diagram for a transmitter-receiver system is shown in figure 6, as introduced in Ziemer's book [4, 454]. Depending on the nature of the arrangement, the system may or may not include the following components: an analog-to-digital converter, an encoder, a digital-to-analog converter.

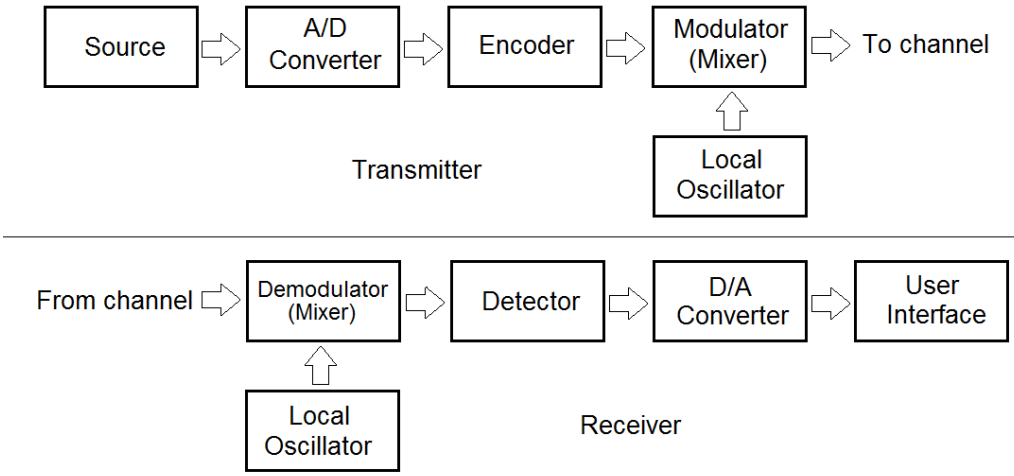

figure 6, Digital transmitter-receiver system

According to figure 6, the source provides the message, which in case of analog signal, is first converter into a digital form. The possible encoding is done to the digital signal but not necessarily. The local oscillator provides a high frequency signal, which is modulated according to message signal in the mixer. The product of the two signals, the carrier signal, is then fed into an antenna which radiates the electromagnetic energy into an air medium.

At the receiver, the order of the blocks is in inverted to gain access to the original message encoded into the high frequency signal. The antenna absorbs the electromagnetic radiation and converts it into an electric signal. The carrier signal is fed into a mixer, which provides the down-converted product between the carrier signal and the local oscillator signal. This product is typically at much lower center frequency than the original carrier signal. The phase variations are detected by the demodulation circuit and converted into a digital mode if needed. Finally the data is transferred into the user interface.

In this project, the PSK-31 carrier signal was at centre frequency of 14.07MHz and the down-conversion electronics were used to bring the signal into a audible frequencies of few kHz. The audible signal was fed into a computer soundcard input for demodulation.

The most common type of antenna implemented in PSK-31 is a dipole. A dipole has a relatively low directivity and is able to cover a good amount of spherical space around the axis of the antenna. A typical representation of the power concentration circles (lobes) of a half-wave dipole (λ/2-dipole) is shown in figure 7 as it was introduced in Räisänen's book [5, 162].

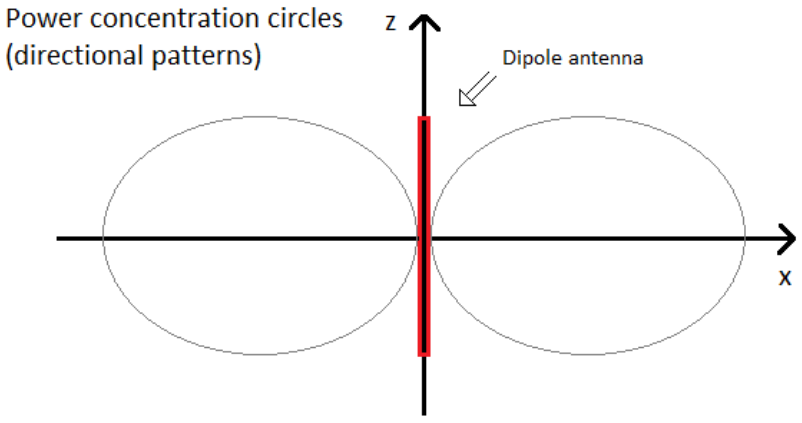

figure 7, Directional pattern of λ/2-dipole

The dipole antenna in figure 7 is observed from above the antenna, so that the axis of the antenna lies on the z-axis. The direction of the power concentration forms two circles on both sides of the antenna. Because of antennas' reciprocal properties, the highest efficiency for the transmission, as well as for the reception, is located along the x-axis.

Transmitting radio signals at a very low power challenges the designer to utilize an antenna optimized for a given frequency and having minimal losses. Antennas of low directivity can receive signals from multiple directions and are good for general situations, whereas antennas with high directivity have very distinctive lobes at certain directions and can concentrate the power inside a very narrow space but can therefore only receive signals that are coming from that direction. For this project it was sensible to select an antenna with low directivity in order to cover as much of the spherical space around the antenna as possible. Simple dipole antennas meet these criteria and are cost effective.

The frequency of the desired radio waves determines the length of the dipole. The most useful of the dipole types is the half-wave dipole which has good gain of 2.15dB and directivity of 1.64, while still being reasonable in size [5,162]. These values can be calculated from the properties of a dipole antenna and are presented here only as results.

The PSK-31 user interface and the digital signal processing system are built into the computer software which, together with the computer hardware, encodes and decodes the information. The software allows the user to select the desired centre frequency by "tuning" the software to enable communication on a distinctive channel. The entire spectrum (around 14MHz) is presented as a waterfall which continuously flows downwards as more data is being encoded. The intensity of the colour in the waterfall indicates the activity on that part of the spectrum, as can be seen in figure 8. The channels are divided by approximately 30Hz. The software called DigiPan [6] was utilized for the digital signal processing and to provide the user interface.

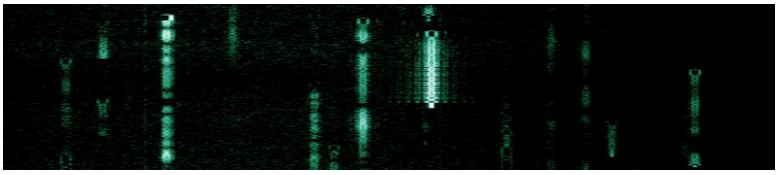

figure 8, PSK-31 waterfall example [2]

3 Receiver Design

3.1 Overview

Like any electronic device, a radio frequency receiver can be considered as an ensemble of separate blocks of functions that are designed to work together to perform distinctive tasks, such as reception, processing and analysis. The project concentrates on the study of the blocks inside the receiver unit. External blocks such as antennas, cables, power supplies and the user interface are usually ready-made and can be bought from dedicated stores to match the desired criteria. The receiver electronics are placed between the antenna and the computer. The project block diagram is represented in figure 9.

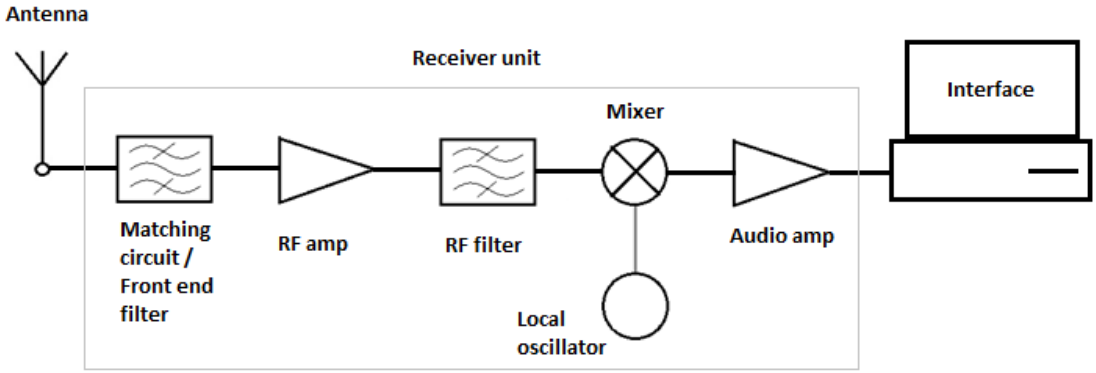

figure 9, Receiver block diagram

The internal electronics of a receiver unit can be designed to process the electronic signal in countless of ways. The level and method of signal processing depends always on the application and can span from simple filtering to extremely complicated modulations. The main purpose of the receiver unit electronics in this project was to amplify the received low-level signal, filter unwanted signals and noise, down-convert the high-frequency signal into audible frequencies by injecting another, lower frequency signal into the channel and to output an audible signal through an audio cable into a computer soundcard for digital signal processing. The actual demodulation of the message is completed by DigiPan [6] software which displays the results through an user interface.

The block diagram shown in figure 10 illustrates the signal processing from the antenna to the interface. The signals shown in the figure represent only "high" and "low" frequency signals and are not in scale with each other.

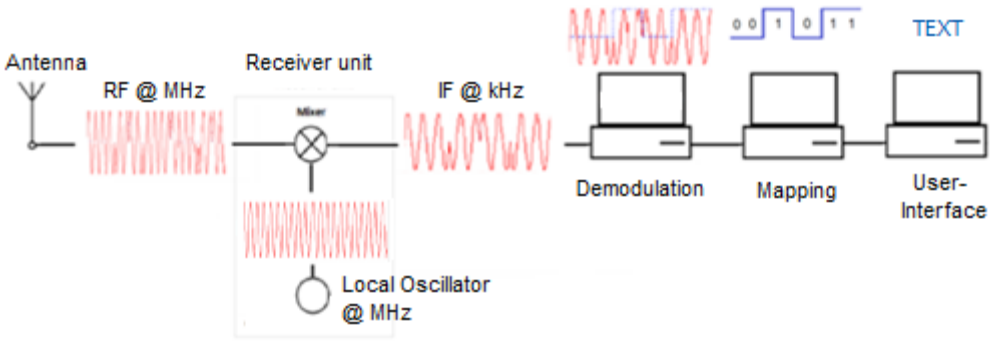

figure 10, Receiver end signal modulations

The local oscillator provides the high frequency signal for down-converting the high frequency RF signal into audible frequency. The conversion is done inside the receiver unit with a mixer which is designed two mix the two signals together and to produce a mathematical product as a results, the IF.

3.2 Antenna

Transmissions using PSK-31 cover a wide range of frequencies from 1.8kHz (160m band) to 28MHz (10m band). Different types of antennas exist and if only a particular frequency is of interest, the antenna can be selected to absorb only a desired spectrum. The antenna for this project was chosen to cover a wide a range of frequencies from 40m band to 10m, having the priority band of 20m in the middle of the reception range. Because of the antenna's wide range, the receiver was to include good filtering electronics. The chosen antenna was of type 10m-40m G5RV and is shown in figure 11.

figure 11, G5RV antenna

G5RV includes a dipole flat-top consisting of two, 7m long stainless steel wires, a 4.5m impedance matching section of a twin lead construction, a balun for RF interference blocking and a female UHF connector (SO239) . The dimensions of the antenna are shown in figure 12.

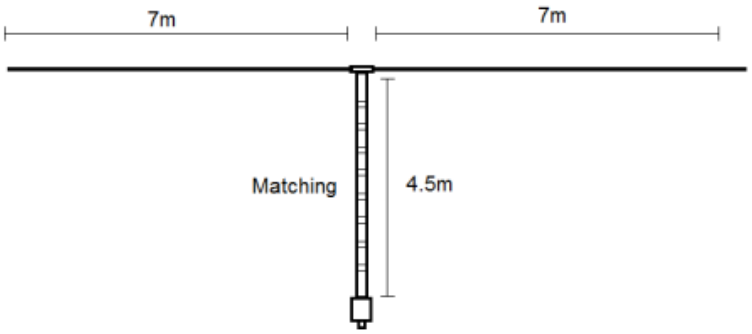

figure 12, G5RV dimensions

The copper wires at the matching section are separated by an isolating plastic material that keeps the wires at a constant distance from each other. Because the antenna is meant to be placed outside, the matching section and the connector are sealed to withstand various weather conditions. [7]

3.3 Receiver Circuit Overview

The goal of the project was to examine the properties on which the PSK-31 receiver operates and the reasoning behind the original design [1]. The theoretical, block-by-block design is introduced in the following chapters, beginning at the front-end filter and ending up to the audio amplifier. The PSK-31 software used during the testing procedures is also covered in the final section of chapter 3. The theoretical part of this report includes calculations, graphs and figures that are based partly on literature sources for general cases. The represented simulations and graphs were plotted using the following computer programs: Multisim, MathCAD, Pads Logic, Pads Layout, Windows Paint and Microsoft Excel.

The circuit design for PSK-31 receiver was done in systematic way to allow the identification of the different, operational parts easily. The original schematic was redone with Pads Logic, circuit diagram design software, to represent the project more accurately and to include all the values and component labels that were used in the design. The

complete version of the schematic can be found as appendix A and the concise version is shown in figure 13.

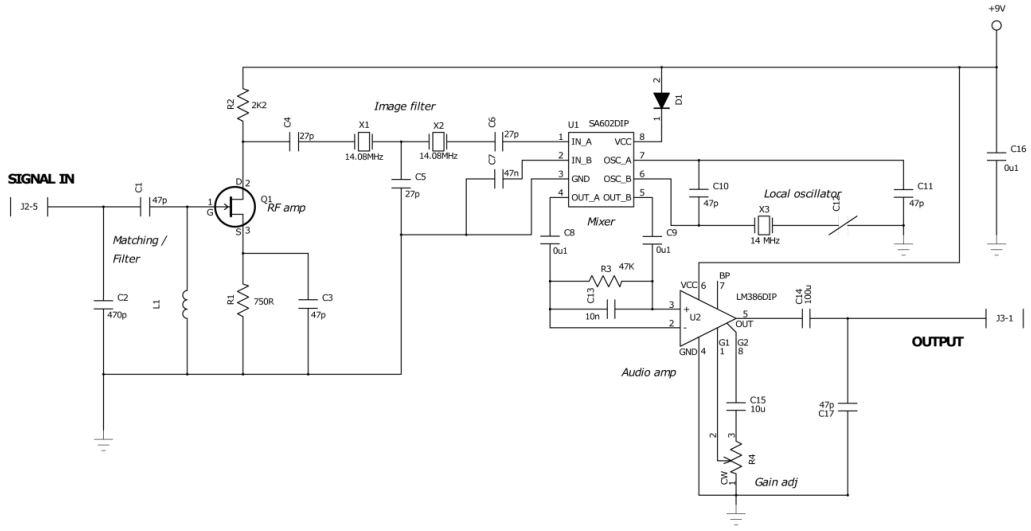

figure 13, PSK-31 receiver schematic for 20m band

According to figure 13, the connector "SIGNAL IN" on the left side of the schematic is the input of the receiver circuit and connects the antenna to the circuit through an SMA/UHF adaptor. The first filter located on the left side of the schematic is the front end filter and is composed of lumped element C1, C2 and L1. The purpose of the front end filter is to attenuate most of the unwanted signals and to act as a matching circuit between the antenna and the radio frequency amplifier. The RF amplifier Q1 is a self-biased, voltage controlled JFET which amplifies the weak, high frequency signal from the antenna to a level required for further processing. The amplification of the JFET is determined by resistors R1 and R2.

The filter between the RF amplifier and the mixer, composed of crystals X1 and X2, is an image rejection filter (or intermediate filter). The IF filter possess a very narrow passband because of the cascaded crystals; the IF filter prevents the image frequency from passing into the mixer along with the wanted signal.

The local oscillator provides the injection frequency to the mixer, according to the frequency crystal X3 and is located on the right side of the schematic. The injection frequency is tunable by means of the variable capacitor C1. The mixer U1 provides two down-converter signals from its differential outputs. These output signals are fed to an audio amplifier U2, which cancels the absorbed noise and raises the signal level to line level, needed for the digital signal processing. The amplifier's gain is controller with the

variable resistor R4. After the final audio amplification the audible signal can be connected to a computer or a speaker via audio cable. The computer software/hardware decodes the signal and maps the symbols to represent actual letters on the interface.

3.4 Front end filter

The filter located in the input of the receiver is called a front end filter. The purpose of the front end is to filter out a wide range of unwanted signals, absorbed into the antenna along with the wanted signal frequency. The front end filter is of bandpass type, having a wide bandwidth and a centre frequency at the wanted signal frequency. In this project the centre frequency was 14.071MHz. The envelope of the filter should not be designed too aggressive in order to keep the attenuation of the desired frequency as low as possible.

With a proper selection of components, the front end filter enables the circuit to act also as an impedance matching circuit between the low impedance antenna output and the high impedance RF amplifier input. Impedance matching is important in radio frequency applications because of the signal's low power at the antenna. It is crucial to have the maximum amount of power transferred from the antenna to the processing circuit, in order to have minimal errors in the output. Matching is also important to avoid the loading of the transmission line between the antenna and the RF amplifier with reflected power. The reflected power can cause so called "standing waves" to appear in the transmission line. A standing wave is a result of a mathematical sum of the actual signal with the reflected signal and represents the maximum and the minimum voltages on the transmission line. If the amplifier is located at these maximum or minimum points, its operation can be seriously compromised. By implementing a proper matching circuit in front of the amplifier, the reflected power can be minimized. The front end filter design for this project is shown in figure 14.

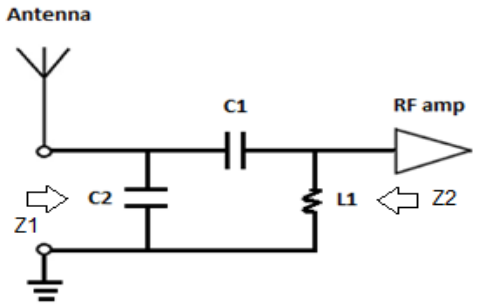

figure 14, Front-end filter

The front end filter was to be designed as a radio frequency resonator, with the resonant frequency matching the wanted input signal frequency of 14.071MHz. A resonator such as this has two resonant frequencies which produce the minimal impedance and the maximum impedance. This is shown in the following calculations. In order to produce maximum voltage drop at the gate of the RF amplifier, the maximum impedance resonance is the desired resonant frequency. The following calculations provide the equations for impedances Z1 and Z2, illustrated in figure 14. The calculations are conducted following the examples found in Sendra/Smith's book [8, 992-993].

Impedance seen by the antenna towards the circuit, Z1:

$$Z_s(s) = \frac{1}{sC_1} + sL_1$$

$$Z_{C2}(s) = \frac{1}{sC_2}$$

$$Z(s) = \frac{1}{\frac{1}{sC_2} + \frac{1}{sL_1 + \frac{1}{sC_1}}} = \frac{1}{sC_2 + \frac{sC_1}{s^2L_1C_1+1}}$$

$$Y(s) = \frac{s^3L_1C_1C_2 + sC_1 + sC_2}{s^2L_1C_1 + 1} = \frac{s^2 + \frac{1}{L_1C_2} + \frac{1}{L_1C_1}}{s\frac{1}{C_2} + \frac{1}{s}(\frac{1}{L_1C_1C_2}} = \frac{s^2 + \frac{1}{L_1C_2} + \frac{1}{L_1C_1}}{\frac{1}{sC_2}(s^2 + \frac{1}{L_1C_1})}$$

$$Z(s) = \frac{1}{sC_2} * \frac{s^2 + \frac{1}{L_1C_1}}{s^2 + \frac{C_1+C_2}{L_1C_1C_2}}$$

$$Z1(s) = \frac{1}{sC_2} * \frac{s^2 + \frac{1}{L_1C_1}}{s^2 + \frac{C_1+C_2}{L_1C_1C_2}} \quad (2)$$

From equation 2, it can be seen that the antenna sees two resonant frequencies that can be solved by analyzing the numerator and the denominator as their values approach zero. The numerator is dependent only on serially connected capacitor and inductor, producing the series resonance at ω_s . The denominator is dependent on the parallel component, producing the parallel resonance at ω_p.

Series resonance at ω_s when $s = j\omega$:

$$\omega_s = \frac{1}{\sqrt{L_1C_1}} \quad (3)$$

Parallel resonance at ω_p :

$$\omega_p = \frac{1}{\sqrt{L_1 \frac{C_1 C_2}{C_1 + C_2}}} \quad (4)$$

Equations 3 and 4 state that the parallel resonance is always larger that the series resonance, $\omega_p > \omega_s$. The difference in the capacitances C_1 and C_2 determine the frequency gap between these two resonant frequencies. Having $C_2 \gg C_1$ the two resonant frequencies are brought closer together. Thus, it is practical to have the two capacitances values rather far apart.

Equation 2 can be expressed in terms of frequency, in order to analyze the modulus the impedance function:

$$|Z(j\omega)| = -j \frac{1}{\omega C_2} * \frac{\omega^2 - {\omega_s}^2}{\omega^2 - {\omega_p}^2}$$

The component selection was done by injecting real component values to the equations and by setting $\omega = 2\pi f_0$, where $f_0 = 14.071MHz$.
The component values were selected as follows:

$L_1 = 2.7\mu H$
$C_1 = 47pF$
$C_2 = 470pF$

The series and parallel resonant frequencies were calculated according to equations 3 and 4, having $\omega = 2\pi f$:

$$f_s = \frac{1}{2\pi\sqrt{2.7\mu H * 47pF}} = 14.128281MHz \qquad f_p = \frac{1}{2\pi\sqrt{2.7\mu H * \frac{47pF * 470pF}{47pF + 470pF}}} = 14.817866MHz$$

The MathCAD calculations for the modulus' and for the graphical representation of the impedance Z1 versus frequency can be seen below in figure 15 and figure 16. The functions utilized in the calculations are based on equations 2, 3 and 4.

$f := 100000, 110000 .. 160000000$

$L1 := 2.7 \cdot 10^{-6}$

$C1 := 47 \cdot 10^{-12}$

$C2 := 470 \cdot 10^{-12}$

$$Z1(f) := \left(\frac{1}{i \cdot 2 \cdot \pi \cdot f \cdot C2}\right) \cdot \frac{(i \cdot 2 \cdot \pi \cdot f)^2 + \frac{1}{L1 \cdot C1}}{\left[(i \cdot 2 \cdot \pi \cdot f)^2 + \frac{C1 + C2}{L1 \cdot C1 \cdot C2}\right]}$$

$$fs := \frac{1}{2 \cdot \pi \sqrt{L1 \cdot C1}} \qquad fp := \frac{1}{2 \cdot \pi \sqrt{L1 \cdot \frac{C1 \cdot C2}{C1 + C2}}}$$

$fs = 1.413 \times 10^7$ $fp = 1.482 \times 10^7$

$f3 := 14.07 \cdot 10^6$ $|Z1(f3)| = 1.831$

$f4 := 14.13 \cdot 10^6$ $|Z1(f4)| = 0.058$

$f5 := 14.82 \cdot 10^6$ $|Z1(f5)| = 7.234 \times 10^3$

figure 15, MathCAD calculations for Z1

The three moduli shown in figure 15 are as follows:

$f_0 = f3 = 14.07MHz \rightarrow \arg Z(f_0) = 1.831\Omega$

$f_s = f4 = 14.13MHz \rightarrow \arg Z(f_s) = 0.058\Omega$

$f_p = f5 = 14.82MHz \rightarrow \arg Z(f_p) = 7.23M\Omega$

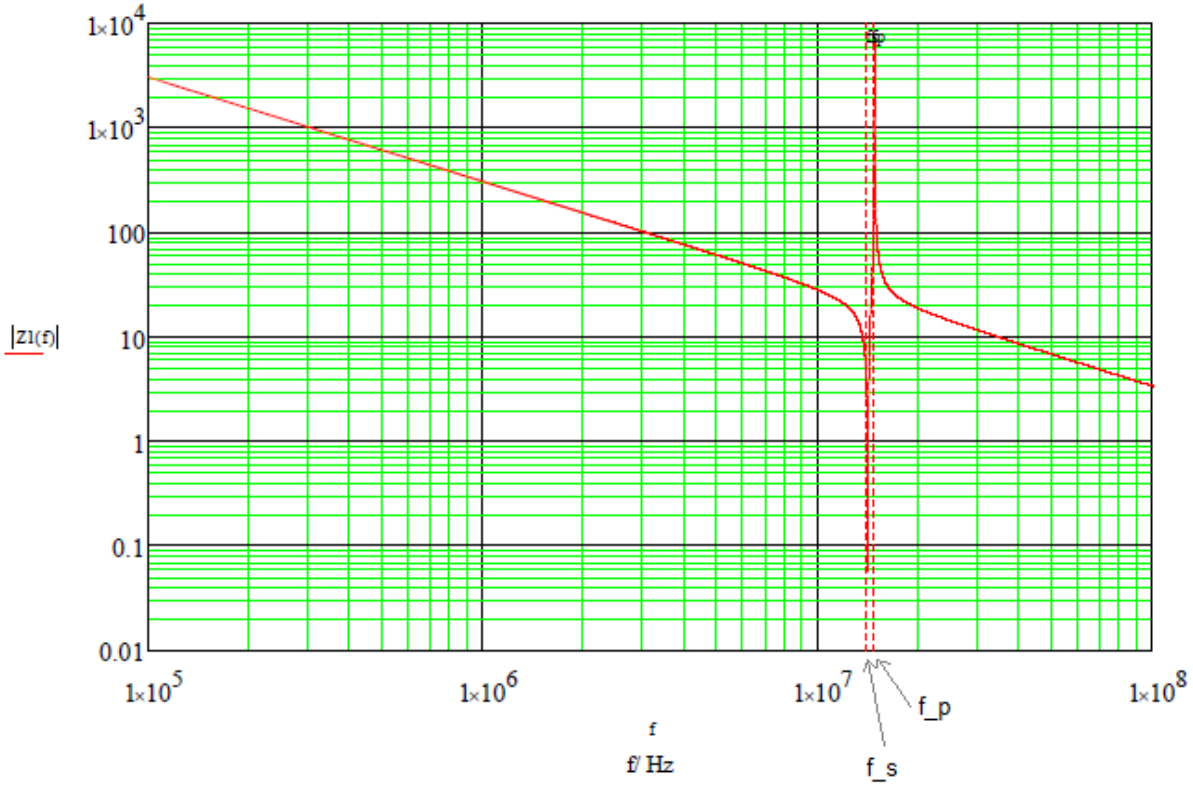

figure 16, Impedance Z1(f), MathCAD

The graph in figure 16 shows the resonant frequencies of the circuit at $f_s = 14.13MHz$ and $f_p = 14.82MHz$, where the impedance dives and rises abruptly. It is imperative to have maximum voltage at the RF amplifier gate, thus the operative frequency of the circuit should be the parallel resonant frequency of the filter. As the theoretical calculations show, the operation of the filter at the actual operational frequency of 14.07MHz is far from optimal, giving a modulus of only 1.831Ω. The limited selection of available component values did not allow a design that would have been optimized at 14.07MHz. Was this a real life application, the design filter should have been forced to have the parallel resonance at the desired frequency. Because of the limited possibilities of available components and time, the filter was accepted as such. It can be shown that by solving the parallel resonant equation for L_1 and injecting 14.07MHz as the desired frequency, the optimal value for $L_1 = 2.995\mu H$.

Impedance Z2, seen by the RF amplifier input towards the antenna, was calculated in the similar way that was shown in the case of Z1:

$$Z_s(s) = \frac{1}{sC_1} + \frac{1}{sC_2} = \frac{1}{s}\left(\frac{C_1 + C_2}{C_1C_2}\right)$$

$$Z(s) = \frac{1}{\frac{1}{\frac{1}{s}\left(\frac{C_1+C_2}{C_1C_2}\right)} + \frac{1}{sL_1}} = \frac{1}{\frac{sL_1 + \frac{1}{s}\left(\frac{C_1+C_2}{C_1C_2}\right)}{L_1\left(\frac{C_1+C_2}{C_1C_2}\right)}}$$

$$Y(S) = \frac{sL_1 + \frac{1}{s}\left(\frac{C_1+C_2}{C_1C_2}\right)}{L_1\left(\frac{C_1+C_2}{C_1C_2}\right)} = \frac{s^2 + \frac{C_1+C_2}{L_1C_1C_2}}{\frac{1}{s}\left(\frac{C_1+C_2}{C_1C_2}\right)}$$

$$Z2(s) = \frac{\frac{1}{s}\left(\frac{C_1+C_2}{C_1C_2}\right)}{s^2 + \frac{C_1+C_2}{L_1C_1C_2}} \quad (5)$$

From the equation 5, it can be seen that from the output port the filter has only one resonant frequency, ω_p which is determined by the denominator and is of same form as equation 4:

$$\omega_p = \frac{1}{\sqrt{L_1\frac{C_1C_2}{C_1+C_2}}} \qquad f_p = \frac{1}{2\pi\sqrt{2.7\mu H * \frac{47pF*470pF}{47pF+470pF}}} = 14.817866MHz$$

3.5 RF amplifier

The role of the RF amplifier is to amplify the received low-level signal to a level which the signal is more convenient to process. The amplification has to be done carefully, keeping in mind the injected noise, an unavoidable phenomenon with any amplifiers Radio frequency amplifiers are often referred as low-noise amplifiers (LNA) because of their good signal-to-noise (S/N). Low-noise amplifiers inject minimal noise into the transmission line as the signal is amplified. Other properties that qualify the amplifier as LNA are bandwidth, noise figure, stability and voltage standing wave ratio (VSWR). The noise figure (NF) measures the degrading of S/N as the signal passes through a portion of the circuit. In case of the RF amplifier implemented in the project (JFET NTE 312) the NF=2dB @ 100MHz [9]. Noise figure of 2dB indicates that the noise is amplified an extra 2dB addition to the normal amplification which includes both the signal and the noise.

The RF amplifier selected in the design is a junction field-effect transistor (JFET). JFET is a voltage controlled semiconductor device, having beneficial characteristics for high frequency and low input power amplifier applications. The high input impedance of a JFET allows no current (in reality minimal current exist) to flow into the controlling gate terminal enabling maximum voltage drop from the gate to source. This is key when the JFET is controlled with relatively low power radio signals. The high input impedance requires a matching circuit between the antenna and the gate terminal in order to prevent reflections and therefore standing waves. The self-biased configuration of JFET can be seen in figure 17.

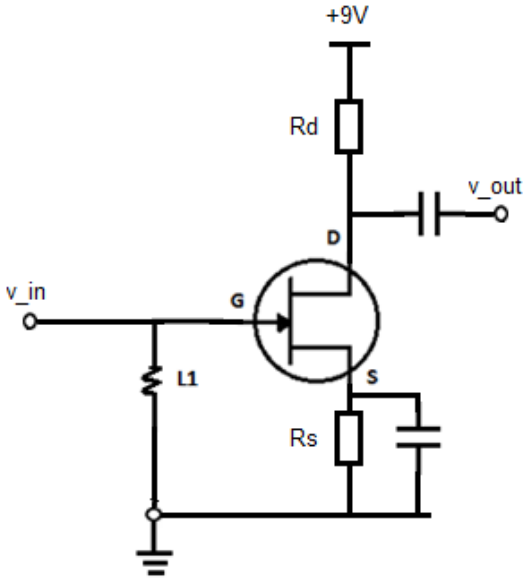

figure 17,Self-Biased, Common-Source JFET configuration

There are two types of JFETs, differentiated by the type of doping used: n-channel and p-channel. The two types differ only on the polarity of the gate-source voltage. JFET is always operated with reverse bias gate-source voltage indicating that for n-channel JFET the gate-source voltage is negative and for p-channel type positive. In JFET implemented in this design is of n-channel type. A typical characteristic curve, and a symbol of n-channel of a JFET is shown in figure 18.

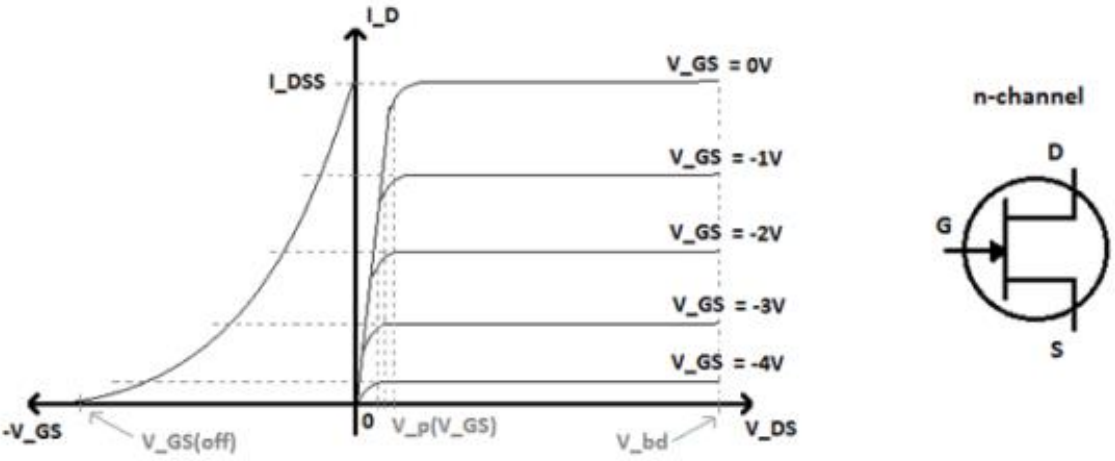

figure 18, Characteristic curve of JFET

The different curves on the right side in figure 18 represent the drain currents at different reverse bias gate-source voltages. Having a selected gate-source voltage, the current through the transistor is fairly constant as the voltage over drain and source is increased. The stable region of a JFET lies between the pinch-off voltage (V_p) and the break-down voltage (V_{bd}). If the drain-source voltage V_{ds} is raised beyond the $V_{bp,}$ the drain-source current I_d increases uncontrollably and usually results into destruction of the transistor. The behaviour of I_d can be expressed as a function of selected $V_{gs,}$ as is shown in following calculations.

The following calculations for JFETs are conducted by following the examples found in Floyd's book [9, 412-435].

$$I_d = I_{DSS}(1 - \frac{V_{GS}}{V_{GS(off)}})^2 \quad (6)$$

The second order polynomial form of the equation (6 is due to the parabolic characteristics of the curve. JFETs are referred commonly as "square law devices" because of the polynomial form of the drain current. Designing JFET amplifiers for exact value of drain current I_d is often problematic because manufactures do not specify distinctive values for I_{DSS} and $V_{GS(off)}$ in datasheets but instead give a range of values.

In case of NTE312 the ranges of I_{DSS} and $V_{GS(off)}$ were given as:

$I_{DSS} = 5mA \ldots 15mA$
$V_{GS(off)} = -1.0V \ldots -6.0V$

This type of range of values produces a family of parabolic curves and makes determining any distinctive values for the source current or the amplification very difficult. One method to approximate the source current theoretically is to take the mid-points of the given ranges. The calculation for I_d is done later in this chapter.

Another important property characterising a JFET is transconductance, g_m. It describes the change of drain current I_d due to the change in gate-source voltage V_{gs}.

$$g_m = \frac{\Delta I_D}{\Delta V_{GS}}$$

The value of transconductance varies on the characteristic curve being larger closer to $V_{GS} = 0V$ and smaller as V_{GS} approaches $V_{GS(off)}$.

In most cases, manufactures provide the value for g_m @ $V_{GS} = 0V$ condition, notated as g_{m0}. To approximate g_m at any point, one can use the equation 7 with the given value of g_{m0}.

$$g_m = g_{m0}(1 - \frac{V_{GS}}{V_{GS(off)}}) \quad (7)$$

Transconductance plays a major role when analysing the amplification of a field-effect transistor. The amplification can be described with the transconductance as is shown below, where R_d represents the parallel circuit of source-resistance and output load-resistance.

$A_v = g_m * R_d$

The very high input impedance is one of the major advantages for using JFETs as amplifiers in high frequency applications. Because JFET is a voltage controlled component and practically no current flows into the gate, JFET has very high efficiency and high isolation between the gate and the source. The input impedance consists of resistance of the channel and reactance due to capacitance in the pn-junction. The capacitance is usually given as C_{ISS} at V_{GS}=0 conditions. The input resistance at the gate can be calculated for a given gate-source reverse current I_{GSS}:

$$R_{IN(gate)} = \left|\frac{V_{GS}}{I_{GSS}}\right| \quad (8)$$

For NTE312 the $I_{GSS} = -1.0nA$ when $V_{GS} = -20V$ producing a following input resistance, according to equation 8 at the gate:

$$R_{IN(gate)} = \left|\frac{-20V}{-1.0nA}\right| = 20G\Omega$$

Having the gate at DC ground through the inductor L1, meaning at 0V, and always at a lower potential than the source because of R1, the JFET is in self-biased mode. This results into having always a negative gate-to-source voltage and the proper operation of the component. In self-biased mode $V_{GS} = -R_s I_D$. When this is substituted into equation (6, the following equation (9 can be derived for the drain current.

$$I_D = I_{DSS}(1 - \frac{I_D R_s}{V_{GS(off)}})^2 \quad (9)$$

The approximation for I_D can be seen below for the given component values:

$R_D = R_2 = 2200\Omega$
$R_S = R_1 = 750\Omega$
$V_{DD} = +9V$

The datasheet of NTE312 give $I_{DSS} = 5mA \ldots 15mA$ thus it is reasonable to assume a mid value of $I_{DSS} = 10mA$. Similarly the value of the cut-off voltage is specified in a range of $V_{GS(off)} = -1.0V \ldots -6.0V$. The cut-off voltage was selected as $V_{GS(off)} = -2.0\text{V}$.

Now the drain current, I_D can be calculated by injecting the values to equation 9.

$$I_D = 10mA\left(1 - \frac{I_D * 750\Omega}{-2.0V}\right)^2 = 1.60mA$$

$I_D \approx I_S$ which results a following the drain voltage, V_D:

$$V_D = V_{DD} - I_D R_D = 9V - 1.60mA * 2200\Omega = 5.48V$$

The gate-to-source voltage, V_{GS} for the given value I_D of is can also be calculated with the approximation of the drain current:

$$V_{GS} = -R_s I_D = -750\Omega * 1.60mA = -1.20V$$

The transconductance is calculated for a given value of gate-to-source voltage of $V_{GS} = -1.20V$ according to equation 7 :

$$g_m = 4mS\left(1 - \frac{-1.2V}{-2.5V}\right) = 2080\mu S$$

Having $g_m = 2080\mu S$ would result having the amplification of 13dB.

An assumption of the characteristic curve of NTE312 can be plotted by assuming the graph as a second order polynomial, obeying a form given by equation 9. The graph with injected values of V_GS(off) =-2.0V, I_DSS=10mA, R_s=750Ω can be seen in figure 19.

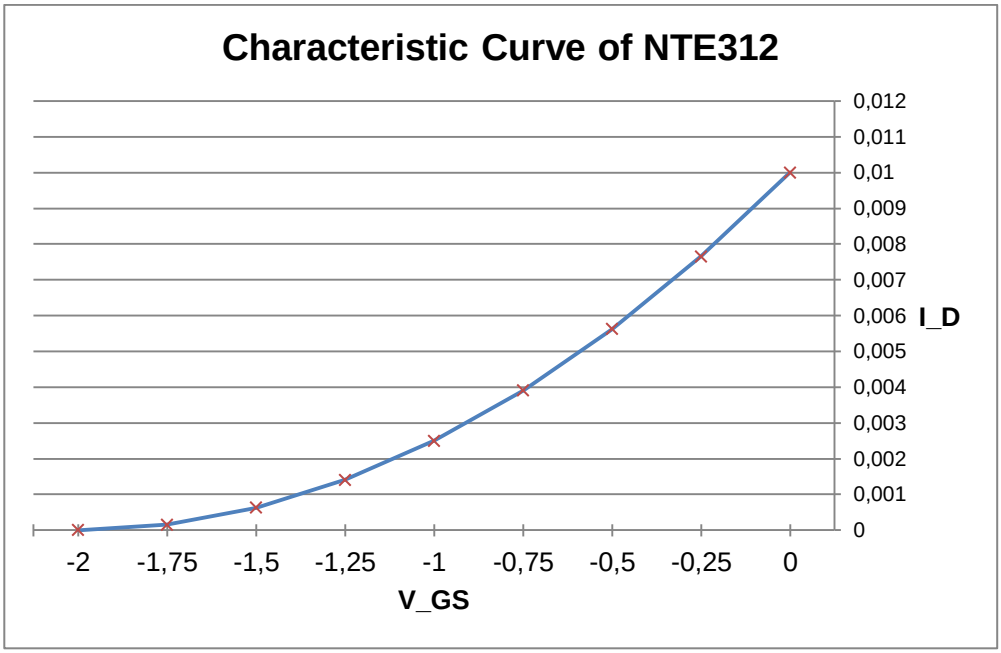

figure 19, Characteristic curve of NTE312 (assumed)

The characteristic curve of NTE312 in figure 19 shows the drain current having much higher values closer the zero gate-source voltage and achieving the maximum at the zero point. The most common and safest configuration of a JFET set the operational point close to the mid-point of the plot. Having I_D close to $\frac{I_{DSS}}{2}$ allows a sinusoidal voltage at the gate to produce safe movement of the drain-current on the plot. For the assumed value of I_{DSS} the mid-point would mean setting $I_D = 5mA$.

3.6 Mixer and Rejection filters

Mixers property to perform a mathematical multiplication of two signals to produce a third one makes them very useful components for radio applications. Mixers are utilized at both, the transmitter and receiver side alike and enable signal conversions required for efficient and reliable transmissions. At the transmitter, shifting a low frequency signal spectrum to a higher centre frequency has several advantages that include the possibility to use smaller size antennas, good propagation through the channel and the possibility for higher data rate. The electronics to up-convert and down-convert signals are relatively simple, making conversions reasonable in almost all applications.

From processing point of view, the high frequency signals are problematic. The receiver end includes a down-conversion section consisting of a mixer and a local oscillator for bringing down the high frequency carrier signal. The mixer multiplies the high fre-

quency signal with the local oscillator signal which results a spectrum shift to a proper centre frequency. The PSK-31 receiver unit performs a down-conversion of a MHz bandpass signal to an audible centre frequency. This project utilises a mixer from NXP Semiconductors of type SA602 [11].

The following calculations and figures follow the examples found in Ziemer/Tranter's book [4, 162-165].

Regardless of the form of modulation, the high frequency carrier can be expressed as shown in equation 10, where x_c is the carrier signal, $A(t)$ is the instantaneous amplitude, ω_c represent the frequency and ϕ(t) the instantaneous phase deviation.

$$x_c(t) = A(t) * \cos[\omega_c t + \phi(t)] \quad (10)$$

Phase-shift keying modulation leaves the amplitude and the frequency of the carrier uninfluenced and touches the phase of the signal only according to the message signal. The message is generally referred as $m(t)$.

Down-converting a signal in frequency means injecting either a higher or a lower frequency signal, x_{LO} from a local oscillator into a mixer with the filtered carrier signal x_c and ejecting a new, intermediate signal x_{IF} for further processing. The intermediate frequency is led through a low-pass filter (intermediate filter) which attenuates the unwanted term and outputs only the desired, down-converted signal $x_s(t)$ as illustrated in figure 20.

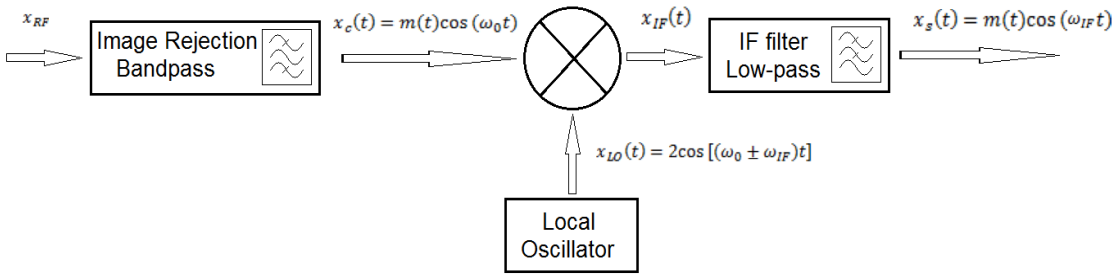

figure 20, Mixer operation

The mixer multiplies the two signals, x_c and x_{LO} together to produce the intermediate frequency x_{IF} as follows:

$$x_{IF}(t) = m(t)\cos(\omega_0 t) * 2\cos[(\omega_0 \pm \omega_{IF})t] = 2m(t)\cos(\omega_0 t)\,cos[(\omega_0 \pm \omega_{IF})t]$$

$$x_{IF}(t) = 2m(t)\frac{1}{2}\{\cos[\omega_0 t - (\omega_0 \pm \omega_{IF})t] + cos[\omega_0 t + (\omega_0 \pm \omega_{IF})t]\}$$

$$x_{IF}(t) = m(t)[\cos(\pm\omega_{IF} t) + \cos(2\omega_0 t \pm \omega_{IF} t)]$$

$$x_{IF}(t) = m(t)cos(\pm\omega_{IF} t) + m(t)\cos(2\omega_0 t \pm \omega_{IF} t) \quad (11)$$

The unwanted term can be seen from equation 11 having spectrum at $2\omega_0 t \pm \omega_{IF}$. The spectrum of the unwanted term is approximately two times the original signal and can be filtered with a low pass filter.

The biggest problem with mixers is their property to frequency shift more than just the wanted signal to the passband of the output filter. As the wanted signal at ω_0 is down-converted to ω_{IF}, so it any signal at so called image frequency $\omega_{img} = \omega_0 + 2\omega_{IF}$. The unwanted signal inside the passband adds noise and causes decoding errors at the signal processing. The down-conversion process, with induced image signal is illustrated in figure 21.

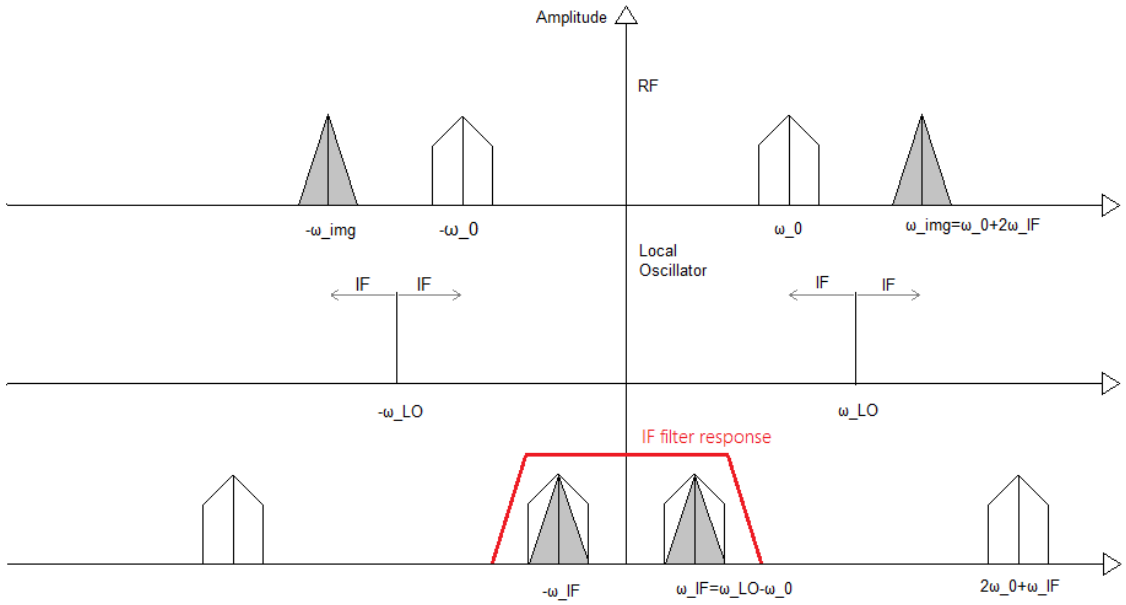

figure 21, Down-conversion and Image frequency problem

The signal at ω_{LO}, shown in figure 21 is applied into the circuit by high-injection so that the local oscillator signal at ω_{LO} is above the carrier frequency ω_0. The spectrum of the carrier signal, along with the image frequency ω_{img} is shifted to ω_{IF} according to equation 11. Because the spectrums lay within the passband of the IF filter, both spectrums are transferred into the signal processing.

To avoid having the image frequency inside the passband of the IF filter, an image rejection filter is utilized before the mixer. The image rejection filter attenuates the spectrum at $\omega_0 + 2\omega_{IF}$, thus removing the unwanted component before it reaches the mixer input. In this project, the image rejection filter was realized by cascading crystals into a crystal ladder structure. This enables a sharp response at the desired spectrum and high attenuation elsewhere, as illustrated in figure 22.

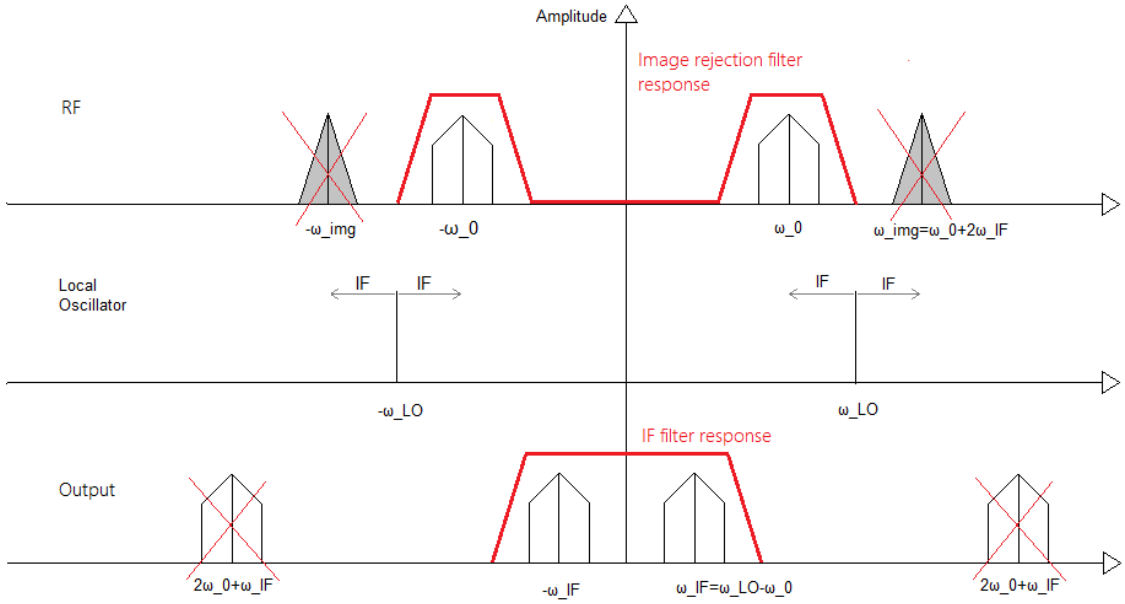

figure 22, Down-conversion with LP-filter

The remaining components are the down-converter message spectrum at ω_{IF} and the "mixer originated spectrum" at $2\omega_0 + \omega_{IF}$. The latter component is attenuated by an intermediate filter. In this project, the IF filter is realized by utilizing the natural properties of an audio amplifier to attenuate all signals outside the audible frequencies.

The characteristics of the image rejection filter can be designed knowing that the image spectrum lies at $2\omega_{IF}$ from the carrier's center frequency. In PSK-31 receiver, where only a specific spectrum at 14.071MHz is wanted, the steep envelope and high attenu-

ation is achieved the easiest by utilizing a quartz crystal resonator as a filter. The ladder structure of the crystal filter is commonly known as a Cohn-type structure. Because of its very narrow passband and high attenuation elsewhere, Cohn filters are also referred as a minimum loss filters for their property to transfer the energy of the signal to the output of the filter with minimal attenuation. The ladder structure of the filter can be seen in figure 23.

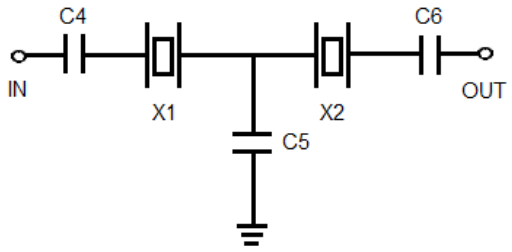

figure 23, IF filter/ Cohn-filter

The frequency response of the Cohn filter is one typical for crystals with both serial and parallel resonant frequencies. The crystal filters are designed to have their natural resonant frequencies at the desired frequency. A Multisim simulation of a frequency sweep from 1kHz to 100MHz, shown in figure 24, illustrates the frequency response of a Cohn filter having two 15MHz crystals and 27pF external capacitors.

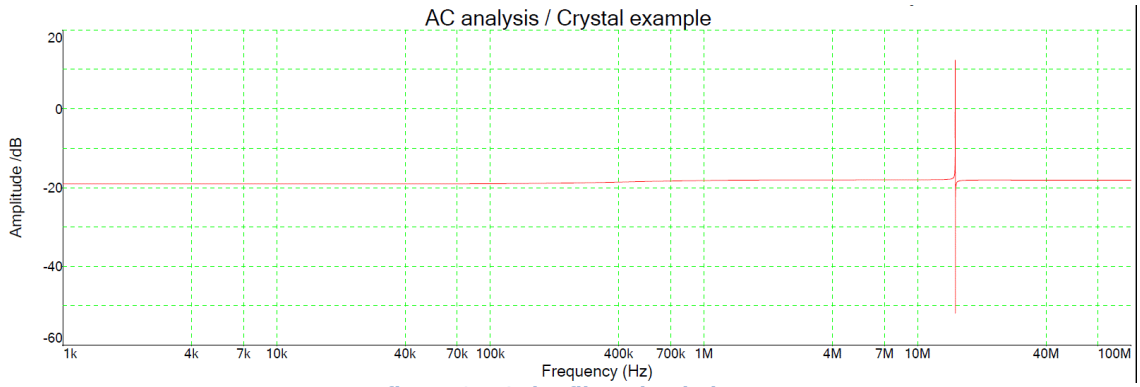

figure 24, Cohn filter simulation

As figure 24 illustrates, all signals are attenuated efficiently outside the narrow passband without the loss of energy inside the filter.

3.7 Local Oscillator

A local oscillator is needed to provide a signal which can be mixer with the carrier signal, in order to down-convert it to lower centre frequency as a intermediate signal. The down-conversion was introduced in Chapter 3.6 and as was stated there, the resulting intermediate signal is the product of the intermediate signal and the local oscillator signal, $x_{IF} = x_c * x_{LO}$.

The resonant circuit can be designed in multiple ways. In order to have a stable resonator which works in variable condition, it is advisable to use crystals. Crystals are both accurate and affordable and liberates the designer from using lumped elements, such as capacitors and inductors.

The frequency of the local oscillator should be a bit higher or a bit lower than the wanted frequency in order to inject the x_{LO} as a low injection or as a high injection. The design for the local oscillator used in this project can be seen in figure 25.

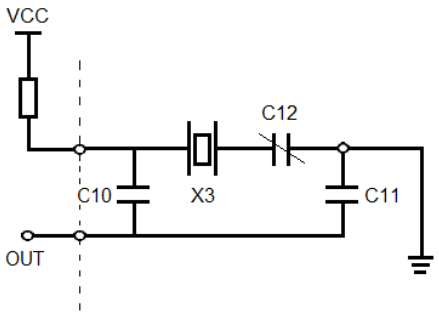

figure 25, Local oscillator circuit

The arrangement seen in figure 25 includes a crystal and a variable capacitor connected in series. This allows a minimal adjustment of the resonant frequency of the crystal and enables the tuning of the local oscillator to produce the correct injection of x_{LO} for the mixer. In this project, the adjustment was in a level of few kHz which is exactly what is wanted to have the carrier spectrum transferred to audible frequency. The simulations for determining the range of the possible frequency adjustment can be seen in figure 26. The simulations were done using Multisim software.

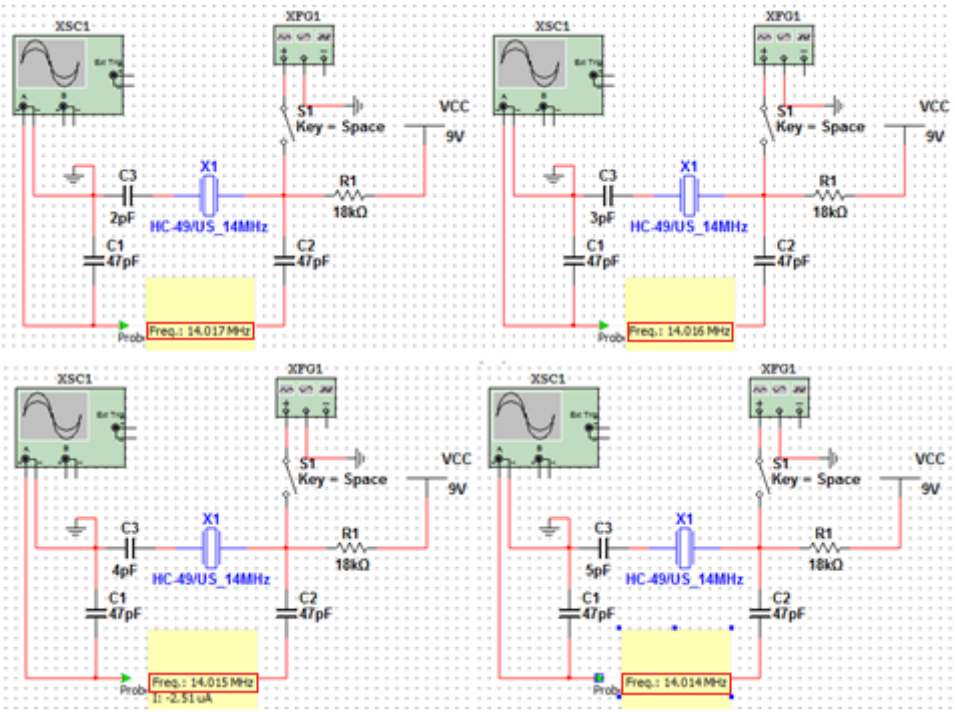

figure 26, Local oscillator frequency adjustment, Multisim

The simulation results show how the crystal's characteristic resonance is achieved with the smallest value of external capacitance and how the frequency rises along with the value of the capacitor. 14.000MHz crystal oscillator can be adjusted approximately 4kHz with 5pF variable capacitor.

3.8 Differential Audio Amplifier

The motivation for using a differential amplifier when dealing with audio signals comes from noise cancellation. A conductor on a circuit board can act as an antenna and pick up external signals from the environment. These signals ad a noise component to the signal and can seriously affect the quality, thus decreasing the signal-to-noise ratio. If the noisy signal is fed into single sided amplifier, both the signal and the noise are amplified. Noise in the signal can cause serious problems in decoding where the components of the signals are mapped to symbols.

The way around the noise is to feed the signal via two signal paths and using a differential amplifier for amplification. The two signal paths carry the same signal but opposite in phase. As before, noise is absorbed into the conductors but this time it is not amplified. Differential amplifier performs a mathematical subtraction of the signals and generates an output signal which is free of the noise and amplitude twice of the original

signals. The principal of noise cancellation of an differential amplifier is shown in figure 27.

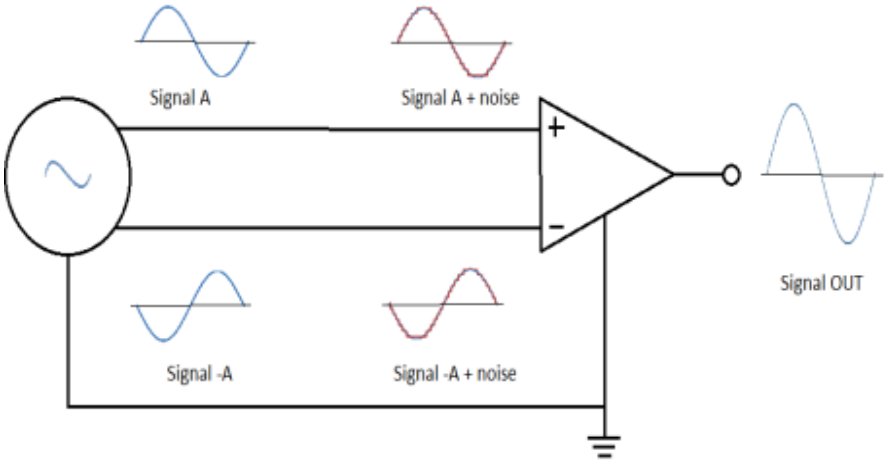

figure 27, Differential inputs and noise cancellation

LM386 [12] was chosen to the final audio amplifier before the output. LM386's gain can be adjusted with external gain control circuit composed of a capacitor and a variable resistor. The gain is internally set to 20dB but can be adjusted with gain control between 20dB and 200dB which is enough for using a small speaker at the output to produce the audible PSK signal.

3.9 Software

The PSK-31 software required for decoding, mapping and to enable user interaction was chosen to be DigiPan 2.0 [6]. DigiPan offers a panoramic view of the spectrum in a form a waterfall view where the simultaneous decoding of all the channels can be observed as the data flows from top to bottom. The decoded messages can be read from the right side of the interface where different channels exist on separate lines. The receiver/transmitter can be tuned simply by clicking a desired channel.

The software is compatible with several phase-shift keying schemes, namely BPSK31, BPSK64, QPSK31 and FSK31. The interface for DigiPan 2.0 is shown in figure 28.

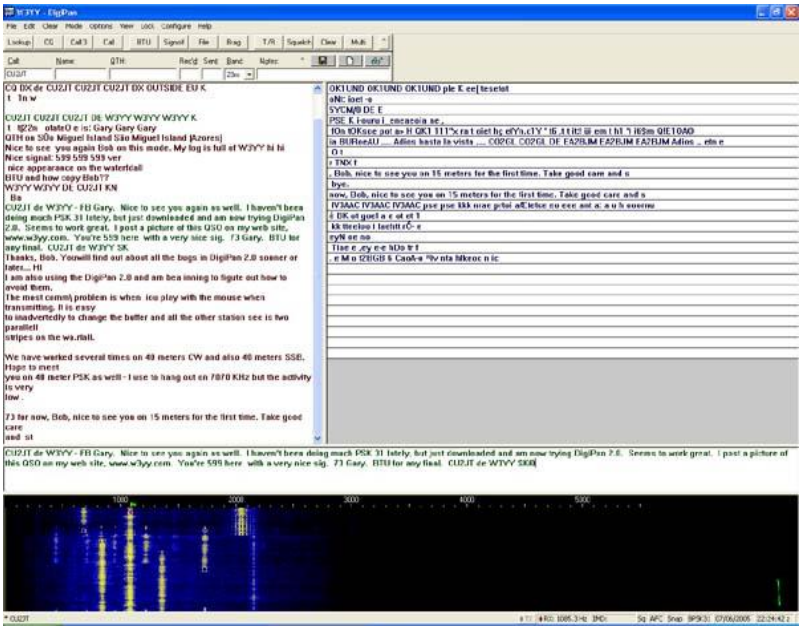

figure 28, DigiPan 2.0 interface

DigiPan 2.0 requires literally no preparations from the user. As soon as the computer soundcard detects an input signal at the right frequency the waterfall appears in the interface and decoding starts. DigiPan 2.0 is freeware software and can be downloaded from its download site: http://www.digipan.net/.

4 Project progress

4.1 Theoretical analysis

The project began by getting acquainted with the original design [1] and by identifying the circuit's building blocks introduced in chapter 3. Many of the concepts used in the circuit design were somewhat familiar but required revising of the previous course materials and many books in the field of radio engineering as well as circuit analysis. The theoretical analysis proved rather challenging and many of the calculations were redone several times to reach satisfactory results. Simulations were done with Multisim and MathCAD software in order to prove the theory was in-line with the circuit design and to show the expected outputs before the actual PCB design.

4.2 PCB design and assembly

The ultimate goal of the project was provide an actual PSK-31 receiver which was to be tested and demonstrated. After gathering enough information on the circuits internal operations, the design process was began with PADS design software. The schematic was redrawn with PADS Logic and was integrated into PADS Layout via program's internal features.

The input and the output of the circuit were situated on the far edges of the PCB to ensure good isolation between the ports. The readability of the PCB was taken into account by constructing block ensembles that were easy to see even without the schematic. The high frequency signals were taken into account by using surface mounted components (SMD) where ever possible and by creating a ground layer on the bottom side of the circuit board. The ground layer was to ensure absorption of noise signals to the ground, thus limiting the nose injection from external sources. The decision to use SMD component instead of conventional through-hole components was for the same reason: to minimize any antenna-like structures in the design. The complete circuit schematic and PCB layout can be found in appendices A and B. The bill of materials is given in appendix C. From the bill of materials it can be seen that the component expenses were around 18€ while the antenna cost approximately 73€.

The milling process was done with Metropolia's LPKF milling machine on a FR4 circuit board. The machine operates together with CircuitCAM and Boardmaster software, allowing user to import milling files from PADS and to configure and control the milling process.

The assembly of the board and the soldering of the components was done with a SMD soldering station which included the required tools for SMD soldering.

4.3 Testing Setup

The test setup was constructed partly in the attic of Albertinkatu campus which was large enough to fit the 10m wide dipole antenna and partly in the electronics laboratory. The antenna was fastened to wooden pillars and a table was used to hold all the equipment. Measurement equipment consisted of multimeters, a voltage source, an oscilloscope and a laptop with DigiPan 2.0 software installed. The measurement setup in the attic can be seen in figure 29, where the receiver is located in the centre of the photo.

figure 29, Measurement setup in the attic

5 Measurements and Results

The assembled prototype can be seen in figure 30. The input is located on the left side of the figure, through a SMA connector. The output is located on the right side, through an 3.5mm audio socket. The front end filter is located next the two crystals along with the JFET acting as an RF amplifier. The green connector on top is the 9V supply voltage with a ground connector next to it. The two crystals, together with the surrounding capacitor, form the IF filter for filtering out the image frequency before the mixer input. The mixer is the left one of the two ICs located at the centre of the picture. The other IC is the audio amplifier. On top side of the audio amplifier is the local oscillator with the crystal and the variable cap on top. Next to the local oscillator is the gain control for the audio amplifier consisting of a variable resistor and a capacitor. The lower capacitor in the figure is the output capacitor.

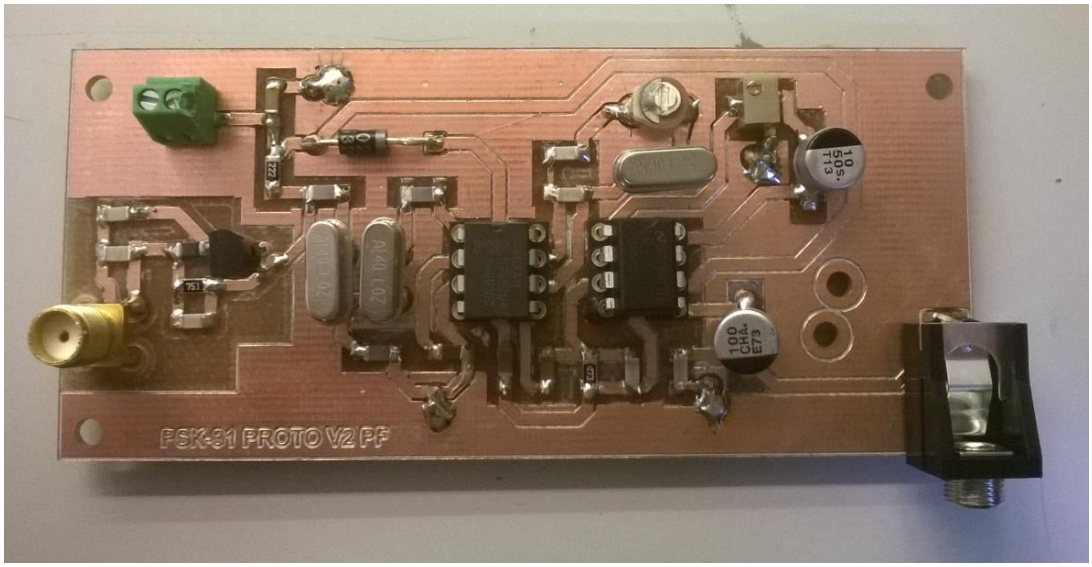

figure 30, Proto PCB

The RF amplifier was measured by connecting the 9V power supply and measuring the voltage values with a multimeter. The measured values of the RF-amplifier in operational conditions are shown in figure 31. The calculations presented in chapter 3.5, based on the NTE321 datasheet values have some deviation from the measured values but provide sufficient accuracy to have confidence in the design.

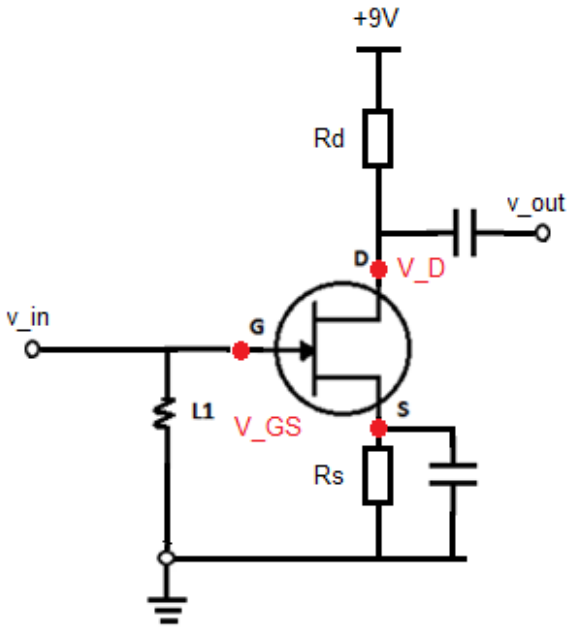

figure 31, RF amplifier measurements

$V_D = 3.59V$

$V_{GS} = -1.76V$

$I_{DSS} = 10.95mA \; @ \; V_{GS} = 0V, V_{DD} = 9V$

Having $V_{GS} = -1.76V$, the amplifier is operating in a relatively good operation point on the characteristic curve, shown in chapter 3.5 as The characteristic curve of NTE312 in and allows safe movement for the gate-to-source voltage and the drain current provoked by the sinusoidal input signal.

After the operation of the RF amplifier was verified the circuit was connected to the antenna and to the laptop to see how the software reacted to the input signal. No input signal was detected at first, as a result of an incorrect tuning of the local oscillator along with the gain control of the audio amplifier. Tuning the circuit made the software display a signal at the waterfall view but because there was only a spectrum at a signal centre frequency, it was obvious the signal was not PSK-31 from antenna but originated inside the receiver. After the circuit was analysed more thoroughly the local oscillator was found as the source of the output signal. The receiver was removed from the testing setup and was brought to the lab for further analysis.

The RF amplifier was tested again and was found operational as before. The next step was to see if the IF filter, composed of two crystals and three capacitors was functioning as intended. For this, the filter had to be insulated from the rest of the circuit by desoldering the three capacitors and by connecting an input signal, from a signal generator to the input capacitor. The output was to be measured with an oscilloscope. Before desoldering, a simulation of the crystal structure was done with Multisim to see if the frequency shift would be possible, even theoretically. The simulation showed that by adjusting the values of the capacitors, the resonant frequency could be shifted approximately 20kHz downwards. Also the losses of the circuit were higher with very low and very high values of capacitors, thus the reasonable capacitor values were around the already selected value of 27pF. For crystals having their natural resonant frequency at 14.089190Mhz, this meant that the series resonant frequency of the filter could be shifter to 14.079MHz. Unfortunately, the desired frequency of 14.071MHz would therefore be filtered out by the crystal filter. Regardless of the simulation results, it was decided to put the theory into test by chancing the real capacitors to different values and by measuring the resulting output. The tested capacitor values were 27pF, 47pF, 470pF and 10nF. All four test circuits were constructed and measured by adjusting the input signal frequency to produce the maximum output. The input signal's peak-to-peak voltage was set to 3.2V in order to have a strong and clear signal. An illustration of the measurement of the filter with 27pF can be seen in figure 32.

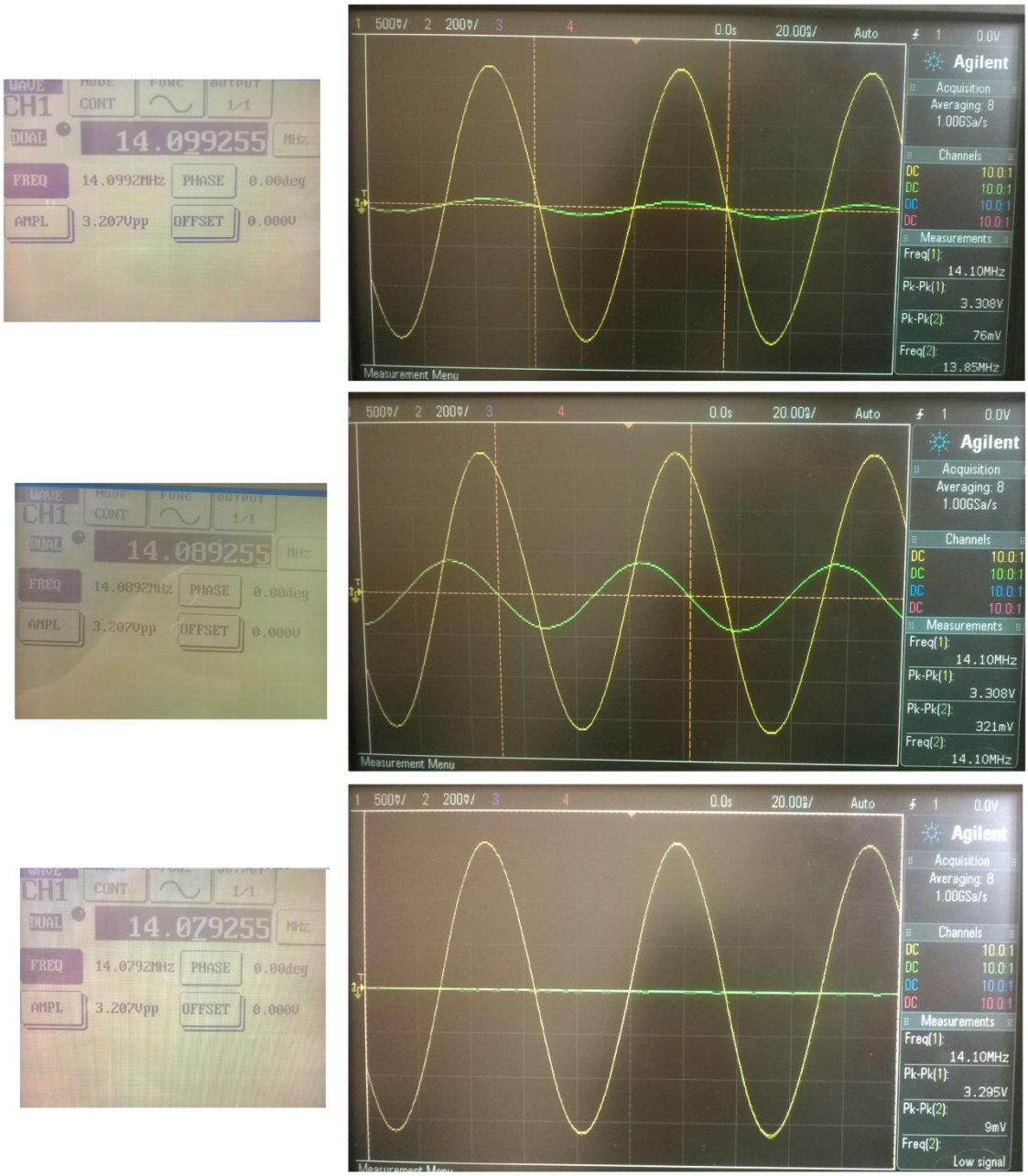

figure 32, Crystal filter measurement (27pF), Input = Yellow & Output = green

In figure 32, the parameters for the injected input signal can be seen on the left. On the right the input signal is illustrated in yellow colour and the output in green. The resonant frequency of the filter with 27pF capacitors was found to be 14.089255MHz. If the yellow colour input signal's frequency is lifted or lowered 10kHz, the green colour output signal drops rapidly. The result agrees with the typical graphical plot of crystal's resonance. The measurement also proves that it is not possible to pass the desired 14.071MHz through the filter. As the capacitor values were swapped to larger values

the maximum shift in the resonant frequency detected with 470pF capacitors which resulted resonant frequency of 14.0839MHz. The downside of injecting larger capacitor values was that the output voltage was now only half of that of the input voltage. This means amplification of -4.74dB. Using 10nF capacitors the resonant frequency remained at 14.0839MHz and the output voltage was decreased even further.

Even when the desired frequency of 14.071MHz was unreachable, because of the crystal filter, the functionality of the mixer was measured. An input signal at 14.0839MHz was injected into the input of the circuit and the two outputs of the mixer were measured with an oscilloscope. The local oscillator was set so that the mixed signals were at approximately 4kHz. The resulting signals can be seen in figure 33 below.

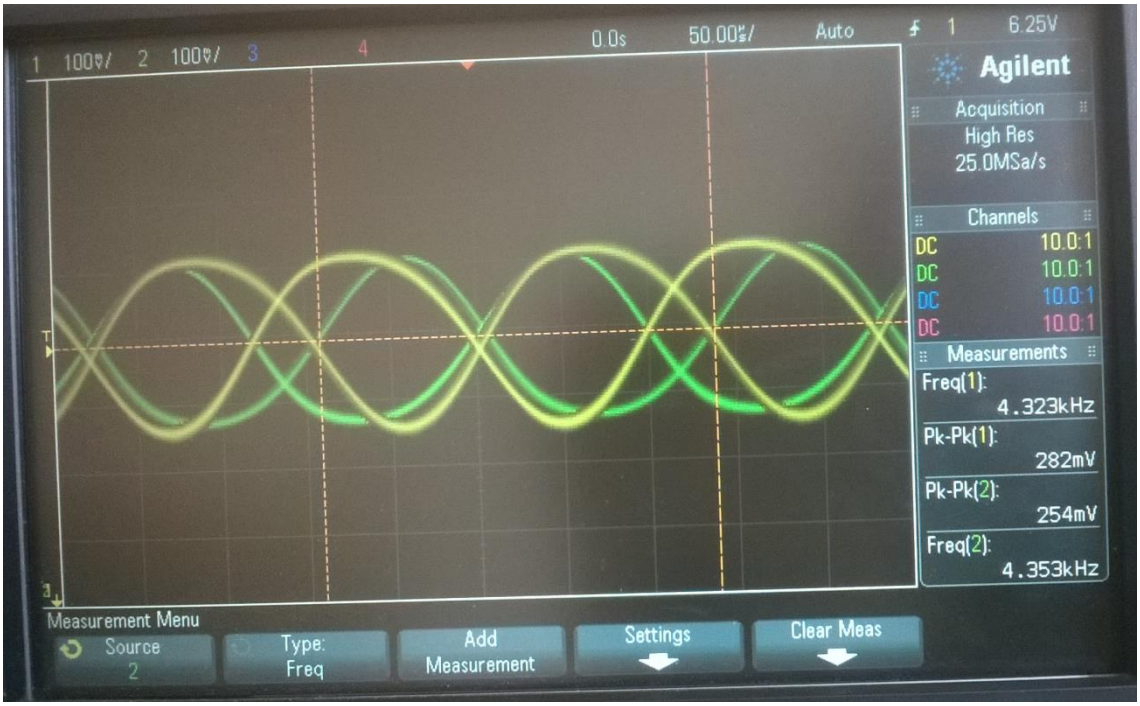

figure 33, Mixer outputs

After the mixer outputs were verified, an oscilloscope was used to measure the output of the entire circuit. By tuning the variable resistor and thus the gain of the amplifier, the output was raised to visual level. The output signal is shown in figure 34. However, the tuning of the local oscillator is not exactly the same as in the setup of figure 33. The output signal was tuned now to approximately 3kHz. The signal had lot of noise and it was therefore difficult to determine the exact frequency.

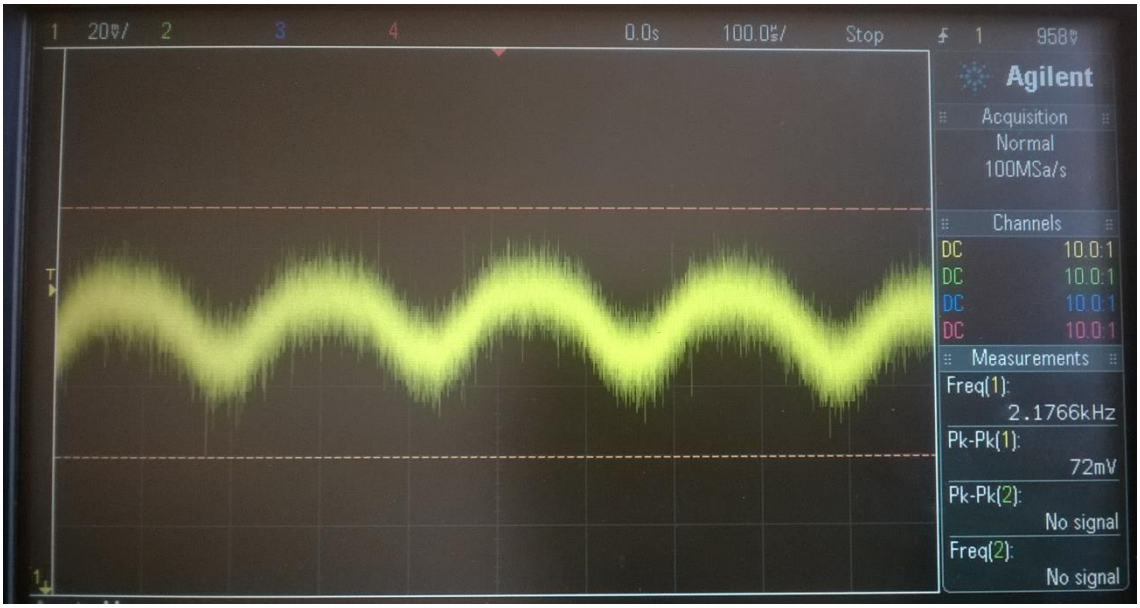

figure 34, Output of the receiver

Next, the output signal, now at kHz range, was fed into the computer's line-in port. The waterfall view in the DigiPan software was utilized to monitor possible input signal. Immediately after the signal was plugged into the computer, via audio cable, the waterfall view displayed a distinctive spectrum at 3kHz (or 14.074MHz) as can be seen in figure 35.

figure 35, Waterfall view spectrum of test signal

This was the farthest point where the project was taken. Several attempts were made to get the circuit to operate with the G5RV antenna but the results were not satisfactory. The reasons most probably lay in the frequency properties the front end filter and the intermediate filter, which were centred at different frequencies because of limited selection on component values.

6 Conclusion and Discussion

This study introduced a circuit design for a PSK-31 receiver for down-converting a high frequency carrier signal to an audible centre frequency. Background information was given on the PSK-31 system by explaining its origins, the utilized modulation schemes and the binary mapping process. The circuit design itself was described by introducing the various elements that make up the complete design. Each element was discussed in a systematic order from the input to the output. Theoretical reasoning was given by explaining the role of each element and their functions as individual blocks. The PCB design and the component selections were based on the various calculations and simulations conducted prior to the assembly process.

The final operation of the circuit can be described as successful in theory as well as in laboratory environment but unsuccessful in field testing. The theoretical reasoning behind the design is solid enough to expect satisfactory results but tends to lean heavily on precise component values of the two filters. The compromises made with the filters resulted into situation where the filters were centred at frequencies that were a bit off from the desired frequency. Because of this, the frequency responses of the filters, at the desired frequency of 14.071MHz caused strong attenuations on the signal. In the laboratory, the input frequency and voltage were adjusted to overcome the attenuations and to force a correct mixer input. This arrangement produced a satisfactory output, at audible frequency of 3kHz. The down-converted output signal was observed in the DSP software, DigiPan. In field testing, with the antenna connected to the circuit, the filters' attenuation of the signal was too large to output a distinctive signal.

Even with the failed field testing, the study of the PSK-31 receiver proved very intriguing and proves just how precise and implicit the receiver design must be, in order to function efficiently. The theoretically determined component values should be transferred as such to the practical implementation and no compromises should be allowed when designing a proper radio receiver.

The analysis of the PSK-31 receiver, presented in this study, provides valuable information for anyone aiming to build a radio receiver. The results can be utilized for various purposes, independent of the transmission type. The original design, entitled "A Universal Direct Conversion Receiver For PSK-31"[1] describes the overall design very well and by slight modification, the circuit can be altered to function as a launch pad for myriad number of receiver types.

7 References

[1] John Post. A Universal Direct Conversion Receiver For PSK-31.
Nutz & Volts; May 2009 [Magazine / Online]
URL:http://www.nutsvolts.com/media-files/A_Universal_Direct_Conversion_Receiver_For_PSK-31.pdf

[2] Peter Martinez. PSK31: A new radio-teletype mode with a traditional philosophy. RADCOM; Dec 1998, Jan 1999 [Magazine / Online]
URL: http://det.bi.ehu.es/~jtpjatae/pdf/p31g3plx.pdf

[3] Wikipedia, The Free Encyclopedia. PSK31 [Online].
URL: http://en.wikipedia.org/wiki/PSK31
Accessed 6 March 2014 (Edited 18 March 2014).

[4] Ziemer, Tranter. Principles of Communications. 4th.
USA: John Wiley & Sons; 1995

[5] Räisänen, Lehto. Radiotekniikka. 8th ed.
Helsinki, Otatieto Oy; 2009

[6] DigiPan (2.0). Call signs: KH6TY, UT2UZ, UU9JDR [Software]
URL: http://www.digipan.net/

[7] G5RV Multi-band Antenna [Online, PDF document]
URL: http://w7sav.net/G5RV.pdf
Accessed 27 March 2014

[8] Sendra, Smith. Microelectronic Circuits. 4th ed.
NY,Oxford: Oxford University Press; 1998

[9] NTE Electronics, "N-Channel Silicon Junction Field Effect Transistor" NTE312. Datasheet [Online, PDF]
URL: http://www.nteinc.com/specs/300to399/pdf/nte312.pdf

[10] Floyd. Electronic Devices. 5th ed.
Upper Saddle River, NJ: Prentice-Hall; 1999

[11] NXP Semiconductors, "Double-balanced mixer and oscillator" SA612A. Datasheet, Sep 1990 (Revised Nov 1997) [Online, PDF].
URL:http://www.alldatasheet.com/datasheet-pdf/pdf/18894/PHILIPS/SA612A.html

[12] Texas Instruments, "Low voltage audio power amplifier" LM386. Datasheet, Aug 2000 [Online, PDF]
URL: http://www.ti.com/product/lm386
Accessed 27 March 2014

[E1] Wikipedia , The Free Encyclopedia.
Bahmer. Atmosphere with Ionosphere. 2007 [Online picture]
URL: http://en.wikipedia.org/wiki/File:Atmosphere_with_Ionosphere.svg
Accessed 27 March 2014

[E2] Wikipedia, The Free Encyclopedia
ISL. TaiWan Ionospheric Model. 2012 [Online picture]
URL:http://en.wikipedia.org/wiki/File:TWIM%27s_ionosphere_with_time.jpg
Accessed 27 March 2014

[E3] Wikipedia, The Free Encyclopedia
Naval Postgraduate School. Ionospheric layers. 2009 [Online picture]
URL: http://en.wikipedia.org/wiki/File:Ionosphere_Layers_en.svg
Accessed 27 March 2014

[E4] Wikipedia, The Free Encyclopedia. Earth-ionosphere waveguide [Online]
URL: http://en.wikipedia.org/wiki/Earth-Ionosphere_waveguide
Accessed 27 March 2014 (Edited 15 March 2014).

[E5] Wikipedia, The Free Encyclopedia
U.S Government. Skywave. 2013 [Online picture]
URL: http://en.wikisource.org/wiki/File:APN2002-figure1007a.jpg
Accessed 27 March 2014

APPENDIX A: Schematic

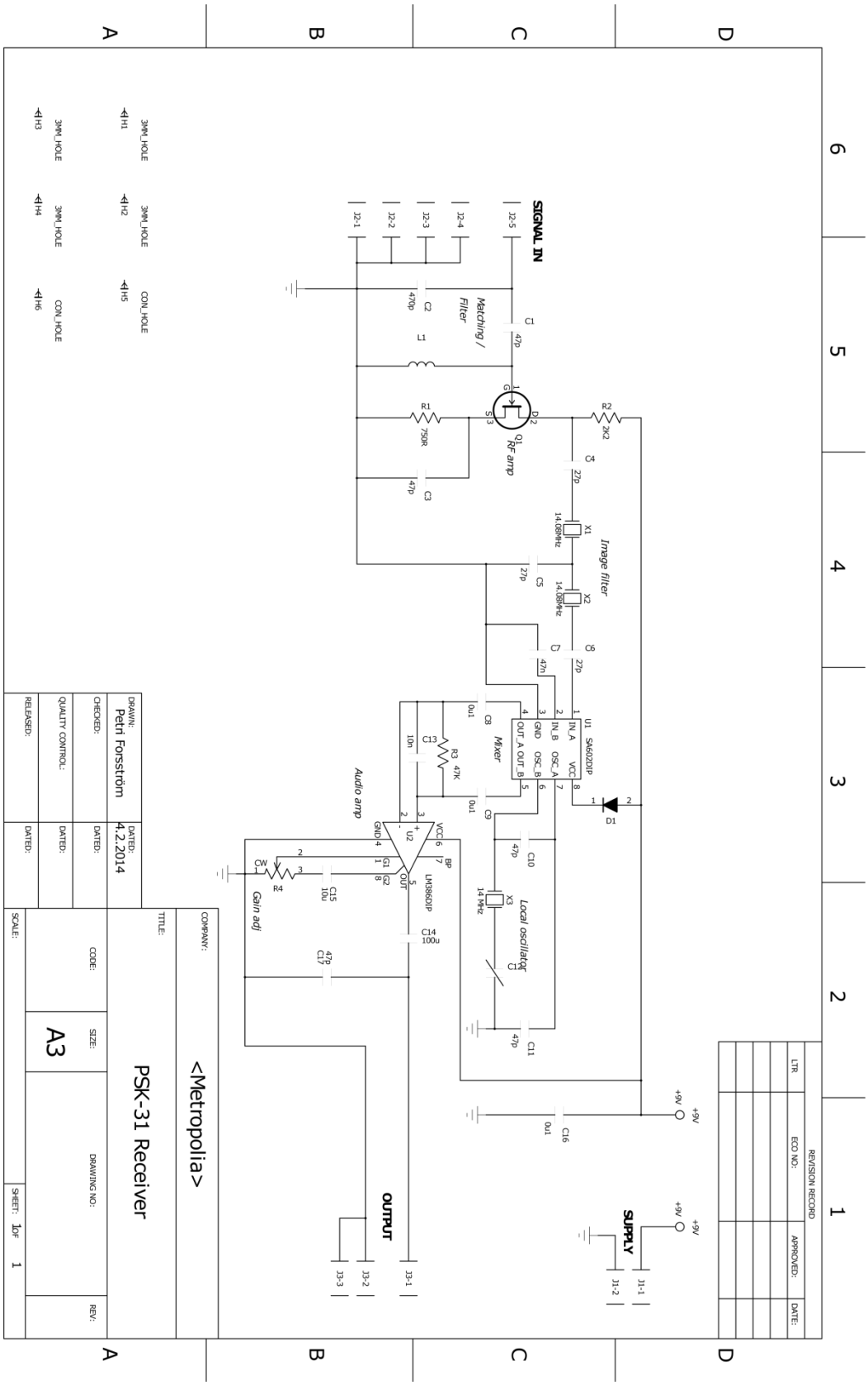

APPENDIX B: PCB Layout

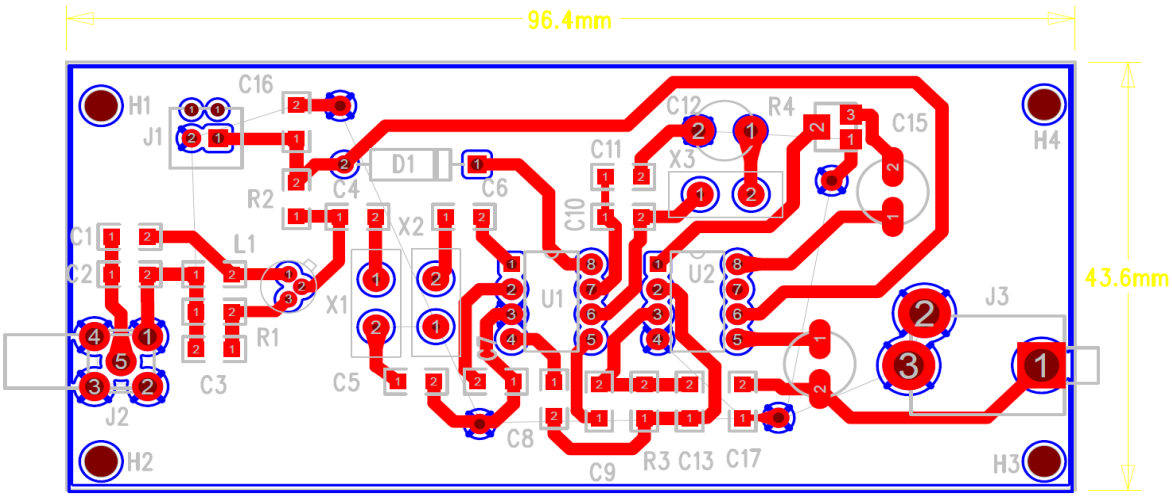

APPENDIX C: Bill of Materials

FARNELL		Quantity	Casing	Description	Manufacturer's code	Manufacturer	Farnell code	Digikey code	price /pcs	price
	Resistors (1/4W, 5%)									
	R1	1	SMD, 1206	750 ohm smd	ERJ8GEYJ751V	Panasonic	2057833		0,02	0,02
	R2	1	SMD, 1206	2.2k smd	ERJ8GEYJ222V	Panasonic	2057845		0,02	0,02
	R3	1	SMD, 1206	47k smd	ERJ8GEYJ473V	Panasonic	2057862		0,02	0,02
	R4	1	SMD, 1206	5k trimmer smd	3214W-1-502E	Bourns	988261		2,26	2,26
	Caps (>16V)									
	C1, C3, C7, C17	4	SMD, 1206	47pF ceramic	CC1206JRNPO9BN470	YAGEO	3606065		0,14	0,56
	C2	1	SMD, 1206	470pF ceramic	CC1206JRNPO9BN471	YAGEO	3606107		0,091	0,091
	C4,C5,C6	3	SMD, 1206	10pF ceramic	CC1206JRNPO9BN100	YAGEO	3606030		0,046	0,138
	C8,C9,C16	3	SMD, 1206	0.1uF ceramic	CC1206KRX7R9BB104	YAGEO	718646		0,066	0,198
	C10,C11	2	SMD, 1206	47pF ceramic	CC1206JRNPO9BN470	YAGEO			0,14	0,28
	C12	1	TH	2.7-10pF trimmer (2.8-12.5pF)	CV05 C1201	Multicomp	1219028		1,46	1,46
	C13	1	SMD, 1206	0.01uF ceramic	CC1206KRX7R9BB103	YAGEO	3606156		0,151	0,151
	C14	1	SMD Radial Can	100uF Electrolytic	EEEHA1C101WP	Panasonic	1973308		0,243	0,243
	C15	1	SMD Radial Can	10uF Electrolytic	EEE1HA100SP	Panasonic	9697110		0,181	0,181
	Inductor									
	L1	1	SMD, 1206	2.7uH	AIML-1206-2R7K-T	Abracon		535-11668-1-ND	0,25	0,25
	Semicon.									
	D1	1	TH DIP8	Diode						
	Q1	1	TO92	JFET	NTE312	NTE	2295728		1,64	1,64
	U1	1	TH DIP8	SA 602 AN mixer	SA602AN	NXP	3026279		3,45	3,45
	U2	1	TH DIP8	LM386 audio amp	LM386N-3	TI	9488340		1,12	1,12
	Misc.									
	J1	1	TH	1/8" phone jack	4832.222	SCHURTER	152206		1,52	1,52
	X1,X2,X3	3	SMD	14.089190MHz crystal	ABLS-14.089190MHZ-10-J4Y-T	Abracon		535-9705-1-ND	0,65	1,95
	J2	1	TH	SMA jack right angle	5-1814400-1	TE	1248989		2,57	2,57
RXTX-tuote										
	Antenna									
	G5RV 40-10m	1	G5RV 40-10m		(RXTX-tuote.fi)				73,8	73,8
									total	**91,92**

APPENDIX D: Skywave Propagation of Electromagnetic Waves

PSK-31 relies on so called skywave propagation where the electromagnetic waves are reflected from the ionosphere allowing intercontinental, wireless transmissions. Ionosphere is a shell of electrons and electrically charger atoms and molecules at reaching altitudes from 85km to 600km from the Earth's surface. The ionization of the atoms is cause by the ultraviolet radiation radiated by the Sun. Ionosphere is included in thermosphere where the atmosphere is so thin that free electrons can exists only for short period of times before they are “captured” by ionized atoms. These free electrons affect the radio wave (electromagnetic radiation) propagation. Because of the ionized atoms the ionosphere consists of plasma where the positive and negatively charged particles are attracted to each other but have so much kinetic energy that they do not form neutral atoms and molecules. The high velocity particles causes high temperatures as they collide resulting the ionosphere being warmer than one that would expect in environment with ions and neutrals. When moving to lower altitudes, gas density increases and since the molecules and ions are closer together the recombination process prevails. The atmospheric layers can be seen in figure 36.

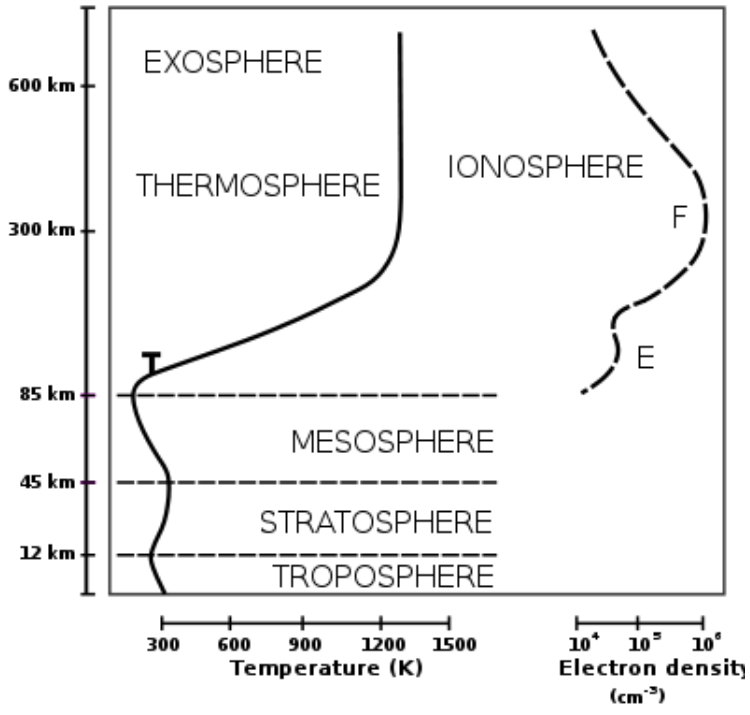

figure 36, Atmosphere [E1]

The ionization effect is related to the amount of radiation from the Sun, thus the effect is much higher on that side of the Earth that is facing the Sun. Also the distance from the Sun has the same effect, thus the ionization is higher at summer time than in winter time. The activity of the Sun (sunspot cycle) varies as well and thus during the high activity period the ionization is again higher and can have unwanted effects on communications on Earth. The ionization is also higher at the equator. The TaiWan Ionospheric Model (TWIM) in figure 37 illustrates how the electron density varies as the time of day progresses.

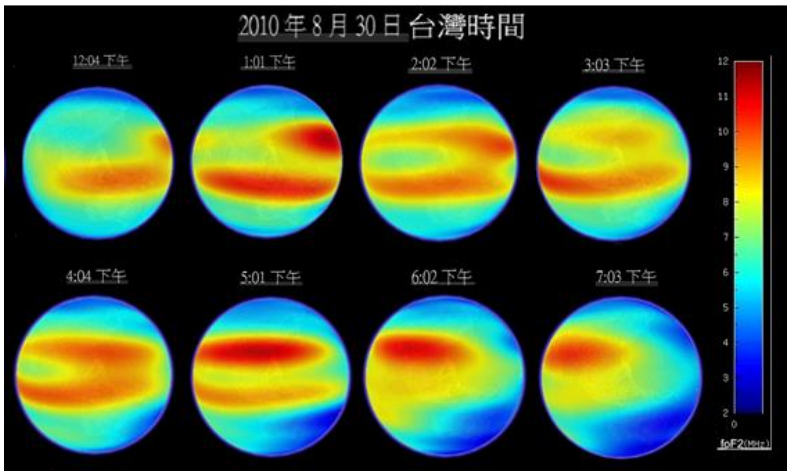

figure 37, TWIM Model of Ionosphere [E2]

The red end of the scale indicates high density of electrons while the deep blue indicates low density of electrons. Research such as this can be used to predict radio propagation.

When electron densities in the ionosphere are examined the ionosphere can be diveded into a several layers that each represent a certain electron density. The order and the sizes of the layers vary and depend on the time of day and time of year. The general representation of the layers can be seen in figure 38.

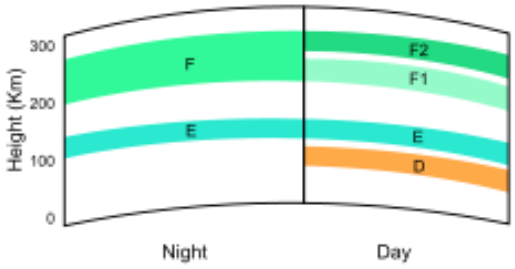

figure 38, Ionosphere layers [E3]

During low radiation period the F layer is the only layer that is heavily ionized. As the radiation increases, layers of ionized gas are introduced in the ionosphere. Most heavily ionized layer during day time is F2 layer. This is the layer that mostly affects the propagation of radio waves. Even though the plasma in ionosphere can be described by electron density, electron and ion temperature and ionic composition the one that is related to the propagation of radiowaves is the electron density. This was shown in figure 37.

As the radio waves reach the ionosphere the electric field of the wave causes oscillations on the free electrons in the plasma. The frequency of these oscillations is the frequency of the radio wave. The oscillating electrons re-emit the original frequency via via electromagnetic wave. The angle of incidence and the frequency of the original electromagnetic radiation effect the re-emitted radiation.

A so called critical frequency exists which defines the highest frequency of the radio wave which tranfers the energy to the free electrons and cause them to oscillate. If the frequency is higher than the critical frequency the free electrons do not have enough time to "respond" (plasma frequency) and the signal will go through the ionosphere without causing emitted electomagnetic radiation. The critical frequnecy can be determined as follows:

$f_{critical} = 9 * \sqrt{N}\ [Hz]$, where $N = \frac{electron\ density}{m^3}$

The Maximum Usable Frequency (MUF) is defined as the upper frequency limit that can be used for transmission between two points at a specified time. The angle of attack affects as follow:

$f_{MUF} = \frac{f_{critical}}{sin\alpha}$

The Earth's surface and the ionosphere can be considered a very large waveguide for extremely low and low frequency signals. One example of this kind of signal that can propagate thousands of kilometers within this waveguide is a lighting strike. This ionosphere has lot of charged particles while the Earth operates as a ground plane. If the frequency is high enough but not higher than the electron plasma frequency of the ion-

osphere the waves are refracted and cause oscillations of the free electrons like described above. If the frequency is higher that the critical frequency the oscillations do not occur and the waves pass to space unaffected.[E4] An illustration of skywave propagation can be seen in figure 39.

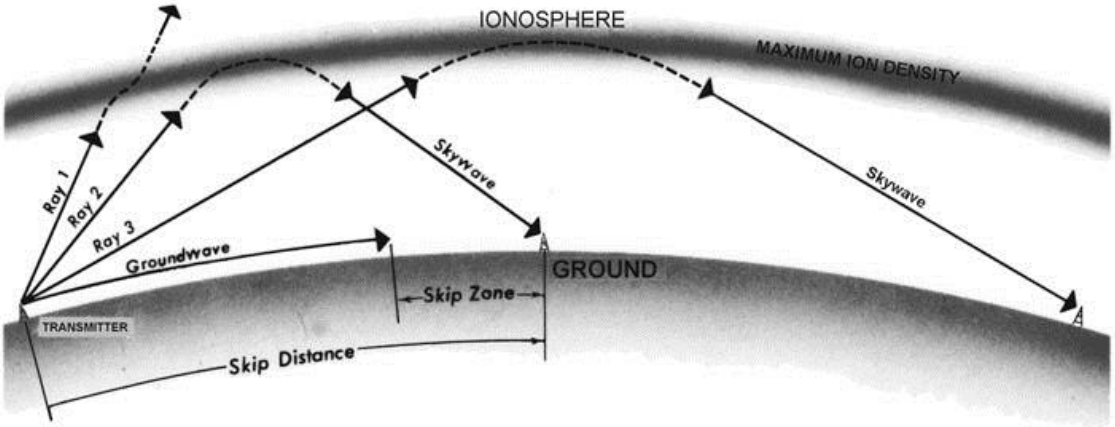

figure 39, Skywave propagation [E5]